Journal Name

ARTICLE

Intracellular delivery of more than one protein with spatio-temporal control

Received 00th January 20xx,
Accepted 00th January 20xx

DOI: 10.1039/x0xx00000x

www.rsc.org/

Miguel M. Lino, Susana Simões, Sónia Pinho and Lino Ferreira*

Transient, non-integrative modulation of cell function by intracellular delivery of proteins has high interest in cellular reprogramming, gene editing and therapeutic medicine applications. Unfortunately, the capacity to deliver intracellularly multiple proteins with temporal and spatial control has not been demonstrated. Here, we report a near infrared (NIR) laser-activatable nanomaterial that allows precise control over the release of two proteins from a single nanomaterial. The nanomaterial is formed by gold nanorods (AuNRs) modified with single stranded DNA (ssDNA) to which complementary DNA-conjugated proteins are hybridized. Using DNA strands with distinct melting temperatures we are able to control independently the release of each protein with a laser using the same wavelength but with different powers. Studies in mammalian cells show that AuNRs conjugated with proteins are internalized by endocytosis and NIR laser irradiation promotes simultaneously endosomal escape and the release of the proteins from the AuNRs. Our results further demonstrate the feasibility of protein release from a carrier that has been accumulated within the cell up to 1 day while maintaining its activity.

Introduction

Intracellular delivery of proteins is extremely useful for the modulation of cellular processes, cell reprogramming and gene editing.[1, 2] In many cases, this type of delivery requires the use of protein carriers to overcome proteins poor membrane permeability. In the past decade, different nanoformulations have been developed to address this need.[3-5] Yet most of these strategies are based on the passive diffusion of the protein from the nanocarrier or on the enzymatic degradation of the nanoformulation.[6] Despite the recent successes in the intracellular delivery of functional proteins,[7-9] so far, no formulation has the capacity to orchestrate the intracellular delivery of more than one protein with remote control. This is an important issue in many biological applications such as cell reprogramming. For example, lineage-switching experiments in the hematopoietic system have shown that the order in which two transcription factors become expressed in a progenitor cell may define the commitment into a given lineage.[10]

Light-sensitive nanomaterials have emerged as an attractive solution to provide spatial and temporal control over the release of molecules within cells.[11] A significant number of light-triggerable formulations that respond to UV or visible light have been described.[12-16] Unfortunately, the UV light has a low penetration depth in biological samples and may exert cytotoxic effects[11]. AuNRs, having a large optical cross section and tuneable plasmon optical resonance in the near infrared range[17], are promising nanomaterials for *in vivo* controlled release of biomolecules. The NIR plasmon resonance band is attractive for biomedical applications due to the "water window" (650-900nm) where there is low light absorbance by skin and tissue. These AuNRs have been mostly used for the controlled release of nucleic acids such as siRNA, small oligonucleotides and plasmid DNA.[18-20] Upon optical excitation, DNA strands hybridized to complementary strands immobilized on the surface of the nanocarrier are released by a photothermal effect.[18, 20, 21] Released siRNAs may mediate gene silencing in model cells.[18]

Although light-triggered release of proteins has been reported,[12, 22] no formulation has achieved the photo-triggered release of more than one protein from the same nanocarrier using a single wavelength. In this work, we have developed a nanomaterial and oligonucleotide chemistry for the intracellular delivery of two proteins with spatio-temporal control using NIR light as a trigger. We further show that the released protein escapes the endolysomal compartment remaining active. Proteins were immobilized on AuNRs by hybridizing complementary single stranded DNA (ssDNA) molecules having different melting temperatures. For the NIR-triggered release we have used a continuous wave (CW) excitation. CW leads to a local increase of temperature creating a gradient from the AuNR core to the bulk solvent, but does not cause cavitation or melting of the AuNR core like pulsed lasers.[23] Although the use of pulsed lasers has been used to induce the cleavage of Au-thiol bonds releasing biomolecules such as siRNA,[24] the selective release of cargos from the same nanocarrier is only possible with CW lasers. The current work opens new opportunities for the intracellular delivery of multiple proteins with spatio-temporal control.

a. CNC, Center for Neurosciences and Cell Biology and Faculty of Medicine, Polo III - Health Sciences Campus University of Coimbra, Rua Larga, 3004-517, Coimbra, Portugal

b.

† Electronic Supplementary Information (ESI) available: Experimental protocols relative to uptake kinetics and AuNR cytotoxicity, intracellular localization of AuNR, immunocytochemistry and endosomal escape. Data relative to the characterization of AuNR and protein-DNA conjugates, sequential release of proteins, AuNR cytotoxicity, uptake and endosomal escape. See DOI: 10.1039/x0xx00000x

Experimental

AuNR synthesis. AuNRs were prepared using the seed mediated method.[25] For the preparation of the seed solution, gold(III) chloride hydrate ($HAuCl_4$, 0.1 M, 12.5 µL) was added to a hexadecyltrimethylammonium bromide (CTAB) solution (0.1 M, 5 mL) and stirred vigorously for 5 min, after which an ice-cold sodium borohydride solution ($NaBH_4$, 10 mM, 0.3 mL) was added. After stirring for 2 min the solution was kept at 25 ºC. For the preparation of growth solution, silver nitrate ($AgNO_3$, 5 mM, 3.2 mL) was added to CTAB solution (0.1 M, 200 mL) and mixed gently, after which $HAuCl_4$ (50 mM, 2 mL) was added. After mixing, ascorbic acid (0.1 M; 1.5 mL) was added. The solution changed from dark yellow to colourless. Finally, 1.5 mL of the seed solution (aged for 8 min at 25 ºC) was added to the growth solution. The solution was kept at 28 ºC for 2 h. The NRs were washed by centrifugation at 9000 g and resuspended in water.

The CTAB on the AuNR surface was replaced using a method already reported with some modifications.[26] Hexanethiol (1.5 mL) was added to the NR-CTAB suspension (2.5 nM; 1 mL). Then, acetone (3 mL) was added and the mixture was swirled for a few seconds. The aqueous phase became clear indicating ligand exchange and the organic phase containing the AuNRs was extracted. Then, a mixture of toluene (2 mL) and methanol (5 mL) was added to the organic phase. The solution was centrifuged at 5.000 g, 10 min, and the pellet was resuspended in 0.5 mL of toluene by brief sonication. The organic to aqueous phase was performed as follows. AuNR-hexanethiol (1 mL) in toluene was added to 9 mL of mercaptohexanoic acid (MHA, 5 mM, 9 mL) in toluene at 95 ºC. The reaction proceeded under reflux with magnetic stirring for 15 min. The precipitation of AuNRs indicated successful coating by MHA. After cooling to room temperature, the aggregates were washed twice with toluene by decantation. Finally, the NRs were washed with isopropanol to deprotonate the carboxylic groups and then the aggregates were redispersed in 1× TBE. The ligand exchange was confirmed by zeta potential measurements.

Functionalization of NR-MHA with single strand DNA (ssDNA). Thiolated ssDNA (sequence A 5'-HS-C6-TTTTTTTTTTTTTTATAACTTCGTATA-3' or sequence B 5'- HS-C6-TTTTTTTTTTTGTCCGGGTCCAGGGC-3', purchased from Sigma-Aldrich) were reduced for 1 h with 100-fold excess of Tris(2-carboxyethyl)phosphine (TCEP) over ssDNA. The NR suspension (0.5 nM; 0.5 mL) was incubated with the thiolated ssDNA for 3 h in a molar ratio of 1:400 in 10 mM phosphate buffer pH 7.4 containing 0.3% (w/v) of sodium dodecyl sulfate (SDS). Afterwards, a NaCl solution (22.5 µL; 0.45 M) was added every 60 min to the AuNR suspension. This operation was repeated four times and the suspension shaked overnight to improve the reaction yield. In the following day, the NR suspension was centrifuged at 9000 g, the supernatant was collected and the pellet was resuspended in 10 mM phosphate buffer with 30 mM NaCl. The amount of oligonucleotides was determined by measuring absorbance at 260 nm in the supernatant. The ssDNA-AuNRs obtained were stored at 4ºC before use (not more than one week).

Labelling of BSA with a fluorescent dye. BSA was labelled with DyLight-NHS ester (Thermo Fisher Scientific). For this purpose, a solution of BSA (2 mg mL^{-1}, 4.8 nmol, in PBS) was mixed with DyLight 488 NHS ester (50 µg, 49.4 nmol) or DyLight 550 NHS ester (50 µg, 48.07 nmol) or DyLight 650 NHS ester (50 µg, 46.9 nmol) and kept under orbital shaking for 2 h. After reaction, the solution was dialyzed against PBS in a dialysis cassette (MWCO 10 kDa) for 48 h at 4 ºC. The final protein concentration and degree of labelling were determined by measuring the absorbance in Nanodrop at 280 nm (A280) and at the DyLight absorbance maximum (Amax; Amax = 493 nm for DyLight 488; 562 nm for DyLight 550 and 652 nm for DyLight 650). The protein concentration was calculated according to the following equation:

$$\boldsymbol{protein\ concentration}\ (\boldsymbol{M}) = \big(\boldsymbol{A280} - (\boldsymbol{Amax} \times \boldsymbol{CF})\big)/\boldsymbol{\varepsilon},$$

where CF is the correction factor (0.147 for DyLight488, 0.0806 for DyLight550 and 0.0371 for DyLight 650) and ε is the molar extinction coefficient of BSA. The number of fluorophores per BSA was calculated from $\boldsymbol{Amax}/(\boldsymbol{\varepsilon'} \times \boldsymbol{protein\ concentration})$

where ε' is the molar extinction coefficient of the dye (70000 M^{-1} cm^{-1} for DyLight 488; 150000 M^{-1} cm^{-1} for DyLight 550 and 250000 M^{-1} cm^{-1} for DyLight 650). After purification each protein had in average 5 fluorophores.

Preparation of protein conjugated with ssDNA. Protein-ssDNA conjugates were prepared using N-[γ-maleimidobutyryloxy]sulfosuccinimide ester (sulfo-GMBS, Thermo Scientific) as linker. Briefly, a solution of protein (BSA-DyLight at 7.5 µM or β-Gal at 3.5 µM in PBS pH 7.4) was reacted with sulfo-GMBS in a 20-fold molar ratio for 30 min at room temperature. The excess of linker was removed by ultrafiltration with Nanosep 30 kDa (Pall Corporation) and the purified protein (7.5 µM; 1.12 nmol in PBS) was reacted with thiolated DNA (22.5 µM; 3.36 nmol in PBS) in a final volume of 150 µL of PBS for 2 h at room temperature. DNA strands were complementary to the strands immobilized on the NR surface (complementary sequence A: 5'-HS-C6-TATACGAAGTTATAAAAAAAAAA; complementary sequence B: 5'-HS-C6-TGCCCTGGACCCGGAC). BSA-ssDNA and β-Gal conjugates were purified by size exclusion HPLC using a Shimadzu-LC-20AD system. β-Gal-ssDNA was purified with a superdex 200 5/150GL column (GE Healthcare) and BSA-ssDNA was purified with a BIOBASIC SEC-300 300 x 7.8mm, 5 µm particle size (Thermo Scientific). PBS was used as eluent at a flow rate of 0.3 mL min^{-1}.

Labelling of NR-ssDNA with TRITC. Thiol-PEG-amine 1 kDa (Creative PEGworks, 20 nmol) was reacted with TRITC (20 nmol) in 1 mL of 10 mM carbonate buffer at pH 9.0 for 2 h at room temperature. Then 500 µL of NR-ssDNA (0.5 nM) were incubated overnight with thiol-PEG-TRITC in a molar ratio of 1:1000. The excess of fluorophore was removed in two steps of centrifugation at 9000 g. The supernatants were then quantified for the presence of TRITC by fluorescence spectroscopy. According to our calculations, we have 540 PEG-TRITC chains immobilized per AuNR. Therefore, the stoichiometry between ssDNA and TRITC in the AuNRs is 1:4.5.

Immobilization of protein-ssDNA conjugates in AuNRs. For the hybridization of complementary oligonucleotide strands conjugated with a protein, a suspension of AuNR-ssDNA (0.5 nM) was incubated with DNA-protein conjugates (150 nM) for 1 h at 37 ºC and then the temperature was slowly decreased to 25 ºC. The excess of DNA-protein conjugate was removed by centrifugation. The amount of DyLight-BSA (DL-BSA) immobilized on the AuNRs was determined indirectly by measuring the fluorescence in the supernatant. The amount of β-Gal immobilized was determined by measuring the enzymatic activity in the supernatant. Briefly, 50 µL of supernatant or NR suspension were added to 100 µL of o-nitrophenyl β-d-galactopyranoside (ONPG, 13 mg mL^{-1} in 0.1 M phosphate buffer pH 7.0) and incubated at 37 ºC for 30 min in a Synergy HT microplate reader. The absorbance at 420 nm was measured every 3 min.

Light-induced release proteins from AuNRs. A suspension of DL-BSA-dsDNA-AuNR (20 µg mL^{-1} in 10 mM phosphate buffer supplemented with 30 mM of NaCl, pH 7.4) was placed in a 96 well plate and irradiated with a fibercoupled Roithner laser (continuous wave at 780 nm) with different laser powers (0.8, 1.25 or 2 W cm^{-2}) placed at 10 cm from the sample. The power of the laser beam in the sample was measured using a thermal power sensor from Thorlabs. After irradiation, the suspension was immediately centrifuged at 9000 g. The fluorescence of the supernatant was measured in order to determine the amount of protein released. To test the multiple release system, AuNRs conjugated with DL_{488}-BSA and DL_{550}-BSA were first irradiated for 2 min at 1.25 W cm^{-2}. The supernatant was collected and after resuspending the pellet, the suspension was irradiated for further 3.5 min at 2 W cm^{-2}.

The light induced release of β-galactosidase conjugated to AuNRs (20 µg mL^{-1} in 10 mM phosphate buffer supplemented with 30 mM of NaCl, pH 7.4) was also studied. For that purpose, after 2 min of irradiation at 0.57, 1.25 or 2 Wcm^{-2}, the supernatant was collected, the pellet was resuspended and the enzymatic activity of the supernatant and the suspension was measured using ONPG as substrate. For that purpose, 50 µL of supernatant or β-Gal-dsDNA-AuNR suspension were added to 100 µL of o-nitrophenyl β-d-galactopyranoside (ONPG, 13 mg mL^{-1} in 0.1 M phosphate buffer pH 7.0) and incubated at 37 ºC for 30 min in a Synergy HT microplate reader. The absorbance at 420 nm was measured every 3 min. The reaction rate was calculated in the linear region of the curve (less than 10% of substrate conversion).

Cell culture. SC-1 mouse fibroblasts were kindly offered by Dr. Carol Stocking. Cells were cultured in 60 mm culture dishes at 37 ºC in a humidified atmosphere of 5% CO_2 in DMEM cell culture media containing 10% fetal bovine serum (FBS) and 0.5% penicillin-streptomycin. Passages 5-25 were used for the experiments; cells were typically grown to 80-90% confluency before splitting and re-seeding 24h before the experiment.

Confocal microscopy. Images were acquired on a Zeiss LSM 710 confocal microscope (Carl Zeiss, Jena, Germany) using a 40x objective/ 1.4 numerical aperture oil PlanApochromat immersion lens. DL_{488} and Lysotraker Green fluorescence was detected using the 488 nm laser line of an Ar laser (25 mW nominal output) and an LP 505 filter. TRITC and Lysotracker Red fluorescence was detected using a 561 nm HeNe laser (1 mW) and an LP 560 filter. DL_{650} and XGal fluorescence was detected using a 633 nm HeNe laser. The pinhole aperture was set to 1 Airy unit. Live cells were imaged at 37 °C and 5% CO_2. Image acquisition and analyses were performed using the Zen Black 2012 software. Fluorescence resonance energy transfer (FRET) was measured by the acceptor photobleaching method [27]. Images were acquired before and after photobleaching TRITC. TRITC was photobleached using the 561 nm laser line with 80% intensity. FRET efficiency was calculated as $FRET_{eff} = [(_{Dafter})-D_{before})]/D_{after}$ x 100 where D_{after} is the fluorescence intensity of the donor (DL488) after acceptor photobleaching, and D_{before} the fuorescence intensity of the donor before acceptor photobleaching. Corrected total cell fluorescence was determined by the subtracting the background fluorescence to the cell fluorescence. The coefficient of variation (CV) of the fluorescence signal was calculated as CV = σ/µ where σ is the standard deviation and µ is the mean. Manders' colocalization coefficient is a measure of pixel overlap, independent of pixel intensities. The value of the coefficient is 1 if all the pixels with fluorescence in the channel (ex. red) overlap with pixels in the other channel (ex. green). A value of zero means that the signal in both channels is mutually exclusive. [28]

Light-induced release of fluorescent BSA in cells. SC-1 cells were seeded in an IBIDI 15 well slide (5000 cells/well), left to adhere for 24 h and then incubated with 50 µg mL^{-1} of AuNR-TRITC conjugated with one fluorescent protein (DL_{488}-BSA Tm 68.9 ºC) or two fluorescent proteins (DL_{650}-BSA Tm 51 ºC; DL_{488}-BSA Tm 68.9 ºC). After 4 h incubation, the medium was replaced and cells were irradiated with a fibercoupled laser (780 nm) at 1.25 or 2 Wcm^{-2} for 2 min. Then, the cells were fixed for 15 min with 4% (v/v) paraformaldehyde and washed three times with PBS. The nucleus was stained with DAPI (1µg mL^{-1}) for 5 min. The release of proteins was studied using the Manders' colocalization coefficient between the fluorescent protein and the AuNR-TRITC. For the dual release experiment, cells were exposed for 4 h to the nanomaterials, washed and then irradiated at 1.25 Wcm^{-2} for 2 min. A group of samples was immediately fixed and the other group was incubated for 5 min at 37 ºC until second irradiation at 2 Wcm^{-2} for 2 min. Then, the cells were fixed for 15 min with paraformaldehyde 4% (v/v) and washed three times with PBS. The nucleus was stained with DAPI (1µg mL^{-1}) for 5 min. The percentage of release of each protein after each stimulus (1.25 Wcm^{-2} or 2 Wcm^{-2}) was inferred from the colocalization between each fluorescent protein and AuNR-TRITC using the following equation: % release = 100 x (MCbefore – MCafter)/MCbefore, where MCbefore is the Manders' colocalization coefficient before each laser stimulus (1.25 Wcm^{-2} or 2 Wcm^{-2}) and MCafter is the Manders' colocalization coefficient after the stimulus.

Light-induced release of β-galactosidase in cells. Enzymatic assay. For the transfection studies with βGal-dsDNA51.7-AuNR, cells were grown in a 15 well IBIDI slide at an initial density of 5000 cells/well for 24 h. After 4 h incubation with βGal-dsDNA51.7-AuNR (50 µg mL^{-1}), medium was replaced and the cells were irradiated with different laser power densities (0.57, 1.25 and 2 W cm^{-2}) for 2 min. After irradiation cells were fixed and the activity of β-Gal was determined with a Senescence Detection Kit (Abcam) following the manufacturer's protocol. After overnight incubation with XGal substrate, cells were observed under confocal microscope. To test the intracellular stability of the released enzyme after laser activation (1.25 W cm^{-2} for 2 min), cells were incubated up to 60

min at 37 ºC until β-Gal activity measurement. To test the stability of internalized AuNRs, after 4h incubation with βGal-dsDNA51.7-AuNR, cells were rinsed with PBS and incubated for 12 h or 24 h before laser irradiation (1.25 W cm^{-2} for 2 min). Immediately after irradiation, cells were fixed and the enzymatic activity was determined as described before.

Transmission electron microscopy (TEM). TEM was used to evaluate endosomal escape of AuNRs. Cells were seeded in a petri dish (60 mm of diameter), left to adhere for 24 h to 90% of confluency and then incubated with DL_{488}-BSA-$dsDNA_{68.9}$-AuNR (50 µg mL^{-1}). After 4 h incubation, the medium was replaced and cells were irradiated with a fibercoupled Roithner laser (780 nm) at 2 W cm^{-2} for 2 min. The culture medium was then removed without allowing the cells to dry. The cells were washed with PBS and 3 mL of fixative (2.5% (v/v) glutaraldehyde in 0.1 M phosphate buffer pH 7.4) was added at room temperature for 45 min by gently shaking. Then the fixative was changed for 0.8 mL of fresh fixative at 4 ºC, the cells were scraped and the suspension was transferred to an Eppendorf. The suspension was centrifuged at 3000 rpm for 4 min at 4 ºC in order to obtain a pellet and 500 µL of fixative were added and left to rest for 15 min at 4 ºC. The fixative was changed by 0.1 M phosphate buffer and the pellet was resuspended. Afterwards the cells were centrifuged at 3000 rpm for 4 min at 4 ºC. The last two steeps were repeated three times in order to completely eliminate the fixative. The samples were then post-fixed with 1% OsO4 0.8% $C_6N_6FeK_4$ in 0.1 M PBS for 2 h at room temperature, washed with PBS 0.1 M, and finally dehydrated (in a graded concentration of acetone). The dehydrated samples were then embedded in resin and sliced in blocs for visualization. TEM images were recorded with a Tecnai Spirit microscope (EM) (FEI, Eindhoven, The Netherlands) equipped with a LaB6 cathode. Images were acquired at 120 kV and room temperature with a 1376 x 1024 pixel CCD camera (FEI, Eindhoven, The Netherlands). Images were acquired with a magnification between 20000X and 80000X. In each image, the number of AuNRs in cell compartments (endosomes, lysosomes and cytosol) was counted and divided by the total number of AuNRs per image to obtain percentage of AuNRs per compartment.

Results and discussion

Preparation of AuNR-protein conjugates

The AuNRs used in this work had an average length of 46.7 ± 4.1 nm and width of 13.8 ± 1.9 nm and showed a plasmon resonance band at 780 nm (Fig. S1a). The AuNRs were coated with ssDNA containing a thiol terminal group at the 5′ end (Supporting Information Table S1) to facilitate the covalent attachment to the AuNR surface (Fig. 1). The two ssDNA tested in this work had a poly-thymine spacer (12 or 15 thymines) followed by an oligonucleotide sequence of 15 or 13 bases, respectively. The poly-thymine spacer was used to keep the oligonucleotide hybridization sequence distant from the AuNR surface.[29] The number of ssDNA per AuNR ranged between 131 and 480 depending on the initial ratio of ssDNA per AuNR (Fig. S1b). The coupling efficiency of ssDNA to AuNR was on average 60% and it was similar for both oligonucleotide strands (Fig. S1b). The hybridization efficiency for the complementary oligonucleotide was above 90%. For subsequent experiments we have used AuNRs with 131 oligonucleotide strands because this number was large enough to immobilize the proteins selected in this study.

For initial experiments, bovine serum albumin (BSA) protein was used as a model protein due to its availability and easily labeling with different fluorescent dyes. The protein was reacted with sulfo-GMBS followed by ssDNA containing a terminal thiol group (protein:ssDNA ratio of 1:2) (Fig. 1). After purification, the protein conjugates had on average 1 ssDNA per protein molecule (Fig. S2). The protein conjugate was then hybridized at 37ºC, using a 300-fold excess of protein over AuNR concentration. Our results show that hybridization of the ssDNA-protein conjugate does not cause significant changes in the absorbance spectrum of the NRs (Fig. S1 b.3). In addition, hybridization of the ssDNA-protein conjugate to the AuNR was not observed when non-complementary ssDNA sequences were used (Fig. S3).

In vitro release of proteins from AuNR-protein conjugates after NIR laser activation

To study the release profiles of proteins, we have used AuNRs hybridized with: (i) $DyLight_{488}$-BSA conjugated with ssDNA with a melting temperature of 51.7ºC (DL_{488}-BSA-$ssDNA_{51.7}$), (ii) BSA-$DyLight_{550}$ conjugated with ssDNA with a melting temperature of 68.9 ºC (DL_{550}-BSA-$ssDNA_{68.9}$), and (iii) both DL_{488}-BSA-$ssDNA_{51.7}$ and DL_{550}-BSA-$ssDNA_{68.9}$ (Fig. 2). Each of the AuNR formulation has approximately 90 BSA molecules per NR. The AuNRs absorb the light and converted it into heat, which then disrupts the physical bonds between the double stranded DNA containing the proteins. BSA release correlated with laser power, i.e., higher concentration of BSA was released from AuNRs exposed to higher laser powers. Approximately 95% and 50% of the immobilized protein was released from DL_{550}-BSA-$dsDNA_{68.9}$-AuNR after a 5 min exposure to a laser power of 2 W cm^{-2} and 1.25 W cm^{-2}, respectively (Fig. 2b).

In addition, for the same laser power, release of BSA correlated with the melting temperature of the ssDNA, i.e., higher concentration of BSA was released from AuNRs conjugated with ssDNA with low (DL_{488}-BSA-$ssDNA_{51.7}$-AuNR) than with high (DL_{550}-BSA-$dsDNA_{68.9}$-AuNR) melting temperature (Fig. 2c).

To demonstrate the dual release of proteins, we have immobilized both DL_{550}-BSA-$ssDNA_{68.9}$ and DL_{488}-BSA-$ssDNA_{51.7}$ in the same AuNR. The samples were irradiated for 2 min at 1.25 W cm^{-2}, centrifuged, the pellet resuspended and irradiated for 3.5 min at 2 W cm^{-2} (Fig. S4 a.1). Our results show that in each laser exposure, one of the proteins got preferentially released (Fig. S4 a.2). The release of the first protein (DL_{488}-BSA-$ssDNA_{51.7}$) was 86%, which is higher than the value achieved in the single protein system. This may be due to a hindrance effect promoted by the other protein (DL_{550}-BSA-$ssDNA_{68.9}$) that is not released by the first stimulus and thus decreasing the possibility of re-hybridization of the released conjugate. Alternatively, a change in the melting transition of the DNA strands in the dual protein system versus single protein system may account for the differences observed.[30]

A recent study has inferred about the stability of proteins released from a NIR-activated Au nanoshell but definitive evidence about its stability was not provided.[12] To investigate whether the photothermal effect observed in AuNRs could reduce the activity of the attached protein, we immobilized a model enzyme, β-galactosidase (β-Gal), in the AuNRs and quantified its activity before and after light activation. The conjugation of β-Gal with $ssDNA_{51.7}$ was not deleterious for the enzymatic activity of β-Gal (Fig. S2c). Each of the NR formulation has a final amount of approximately 5 β-Gal molecules per AuNR due to the large molecular weight of the protein (464 KDa). Enzymatic activity was observed in the released

enzyme (88% activity in the supernatant and 6% in the NR suspension after 2 min at 2 W cm^{-2}, relatively to the initial enzymatic activity), which indicates that the photothermal effect in AuNRs had a minimal impact in the enzyme activity (Fig. 2d).

Uptake and cytotoxicity of AuNRs

Next, we evaluated the interaction of AuNRs with cells. We have selected fibroblasts as a cell model since many of reprogramming protocols used fibroblasts as a starting point.[31] Initially, we evaluated potential cytotoxic effects of AuNRs (we have used BSA-dsDNA$_{51.7}$-AuNR as a model) and light in the cells. AuNRs (up to 50 µg/mL, with or without light activation) and light (up to 2 Wcm^{-2}) alone had a low cytotoxic effect (below 20%) (Fig. S5). Then, we quantified cellular uptake of AuNRs using inductively coupled mass spectrometry (ICP-MS) (Fig. S6). Cells were incubated with AuNRs (50 µg/mL) for different times in DMEM (with 10% FBS), washed and finally characterized by ICP-MS. Each single cell internalized approximately 3.9 pg of AuNRs during the first 4 h (Fig. S6a). Cell uptake of NRs was not substantially improved for exposure times above 4 h. In addition, the intracellular accumulation of AuNRs depends on cell proliferation. If cell proliferation was inhibited with mitomycin C, 75% of the initial content of AuNRs remained in the cytoplasm after 24 h of cell culture (Fig. S6b).

Intracellular release of a single protein from AuNR-protein conjugates after NIR laser activation

To demonstrate the release of proteins within the cell after light activation, fibroblasts were incubated with DL$_{488}$-BSA-ssDNA$_{68.9}$-AuNRs-TRITC (TRITC was attached to the Au core of the NR by a polyethylene glycol linker) for 4 h, washed to remove non-internalized AuNRs and finally activated by a NIR laser with variable power (1.25 or 2 W cm^{-2}) for 2 min (Fig. 3a). Irradiated fibroblasts showed higher fluorescence (in the green and red channel) as compared to non-irradiated cells (Fig. 3b.1). This result confirms the laser-induced release of the protein, which results in less proximity between DL$_{488}$-BSA-ssDNA$_{68.9}$ and AuNRs and a decrease in the quenching effect.[32] Our results further show that an increase in laser power correlates with an increase in fluorescence (i.e. "corrected total cell fluorescence") (Fig. 3b.2), supporting the thesis that more protein is released for higher laser powers. To gain further insights about the release of the protein, the coefficient of variation (CV) of protein signal (Fig. 3b.3) and Manders' colocalization coefficient (Fig. 3b.4) between AuNR-TRITC and DL$_{488}$-BSA-ssDNA$_{68.9}$ were determined. Both Manders' colocalization coefficient and CV of the total cell fluorescence decreased for higher laser powers, which is an indication of protein diffusion in the cells. However, in the non-irradiated cells, the Manders' colocalization coefficient between AuNR and BSA is not 100% probably due to the proximity between TRITC and the AuNR surface, which may result in a quenching of TRITC fluorescence.[32, 33] Therefore, part of the AuNR-TRITC fluorescence is not detected under confocal microscope, decreasing the colocalization coefficient between DyLight and TRITC.

To understand the fluorescence overlap we used the Forster Resonance Energy Transfer (FRET) acceptor photobleaching method (Fig. 4a). This technique measures the donor fluorescence (DL$_{488}$-BSA-ssDNA$_{68.9}$) before and after photobleaching the acceptor (AuNR-TRITC). The efficiency of FRET is mainly based on the donor-acceptor separation distance [34]. If the molecules are close enough (2-10 nm), a resultant increased fluorescence will occur on the donor (DL$_{488}$-BSA-ssDNA$_{68.9}$). Confocal images in fibroblasts show an increase in DL$_{488}$-BSA-ssDNA$_{68.9}$ fluorescence after photobleaching the acceptor (AuNR-TRITC) (Fig. 4b). The FRET efficiency in non-irradiated cells is higher than in irradiated cells indicating that the distance between AuNR-TRITC and DL$_{488}$-BSA in non-irradiated cells is shorter than in irradiated cells. These results suggest that, although the protein and the AuNR core co-localize within cells, the protein is not bound to the AuNR in the irradiated cells.

Next, we studied whether the protein cargo after light activation was entrapped in the endolysosomal compartment or released in the cytoplasm. Fibroblasts were incubated with BSA-dsDNA$_{51.7}$-AuNRs for 4 h, washed, activated or not by a NIR laser (1.25 W cm^{-2}) for 2 min and then fixed. The intracellular trafficking of NRs was then studied by transmission electron microscopy (TEM) (Fig. 5a). In the absence of laser irradiation, BSA-dsDNA$_{51.7}$-AuNRs accumulated in vesicles (almost 90%) specifically in endosomes (67.0% ± 1.0%) and lysosomes (21.2% ± 1.0%). After laser irradiation (2 W cm^{-2}), most BSA-dsDNA$_{51.7}$-AuNRs accumulated in the cytoplasm (57.8% ± 3.4%) while the remaining NRs were entrapped in endosomes (35.7% ± 3.0%) and lysosomes (6.5% ± 0.8%). In a separate experiment, using the previous incubation protocol, we monitored the intracellular trafficking of BSA-dsDNA$_{51.7}$-AuNR-TRITC using an endolysosomal dye, Lysotracker (Fig. S7). In the absence of light, the number of AuNRs in the cytoplasm was 34.8±5.5% (more than observed by TEM; however, this dye might not take into account the AuNRs accumulated in early endosomes [35]) while after laser irradiation, the number of AuNRs in the cytoplasm was 62.4±6.4%.

To further demonstrate that NIR irradiation triggers AuNR endolysosomal escape, fibroblasts were incubated with BSA-dsDNA$_{51.7}$-AuNR in the presence of calcein, a membrane-impermeable fluorophore[36], followed by the incubation with Lysotracker (Fig. S8). Cells treated with AuNRs and calcein, but without NIR laser activation, showed a punctuate distribution of fluorescence indicative of endolysosomal retention of the dye. In contrast, cells exposed to AuNRs and calcein and activated with NIR laser showed a diffuse signal (confirmed by the fluorescence profile plots) of the calcein in the cell cytoplasm and a decrease in Manders' colocalization coefficient between calcein and endolysosomal compartment. Both results indicate that calcein escaped the endolysosomal compartment (Fig. S8). It is possible that endosomal membrane damage by radical species generated by AuNRs after NIR laser activation[19, 37, 38] favors the escape of calcein from endolysosomal compartment.

Intracellular release of two proteins from AuNR-protein conjugates after NIR laser activation: functional activity and temporal control of release

To investigate the intracellular delivery of two proteins within cells with temporal control, we have immobilized both DL$_{650}$-BSA-ssDNA$_{51.7}$ and DL$_{488}$-BSA-ssDNA$_{68.9}$ in AuNRs conjugated with TRITC followed by their incubation with cells for 4 h. Cells were then washed, activated with a NIR laser and fluorescence (co-localization of AuNR-TRITC with each fluorescent protein; see experimental section) monitored by a confocal microscope (Fig. 5c). The first stimulus (1.25 W cm^{-2}, 2 min) induced primarily the release of DL$_{650}$-BSA-ssDNA$_{51.7}$ while the second stimulus (2 W cm^{-2}, 2 min) induced primarily the release of DL$_{488}$-BSA-ssDNA$_{68.9}$. After the 2 stimuli the total of each protein released was lower than 50% likely due to the

spatial confinement in the endolysosomal compartment and potential re-hybridization.

To show the capacity of AuNRs to deliver a functional protein to cells, we used β-Gal as a model enzyme. Fibroblasts were incubated with β-Gal-ds$DNA_{51.7}$-AuNR for 4 h, washed, and then activated by a NIR laser with variable power. The activity of β-Gal was immediately measured by confocal microscopy using a fluorescent substrate[39] (Fig. 6). Irradiated cells showed a higher fluorescence and thus a higher intracellular enzyme activity (Fig. 6 a.2). When denatured β-Gal was used, irradiation did not induce significant changes in fluorescence (Fig. S9). We attributed the increase of enzyme activity to a change in the intracellular localization of the enzyme. With laser irradiation, it is expected that most of enzyme and AuNR escape the endolysosomal compartment (see before) to the cytosol. The pH conditions (pH ≈ 7.2[40]) in the cytosol favours an increase in enzyme activity as compared to the pH conditions in the endolysosomal compartment (pH between 6.3 and 5.5 [40]) (Fig. S10). Moreover, irradiated cells showed a lower co-localization between the enzyme and the AuNR by immunofluorescence (Fig. S11) suggesting the release of the enzyme from the AuNR.

Next, we evaluated the possibility of controlling the release of the protein from the AuNR accumulated within the cell for at least one day. Therefore, cells were incubated with β-Gal-ds$DNA_{51.7}$-AuNR for 4 h, cultured for additional 24 h and finally activated by a NIR laser (1.25 W cm^{-2}, 2 min). Irradiated cells showed a higher fluorescence, and thus a higher intracellular enzyme activity, than non-irradiated cells (Fig. 6 a.3). This indicates that protein carriers may accumulate within cells for at least 1 day without decreasing significantly the enzyme activity. It is likely that β-Gal benefits from a protective environment against proteolytic degradation while immobilized on the AuNRs.

Overall, our results demonstrate temporal control in the release of proteins as well as their functional activity within cells. Previous studies have demonstrated the release of siRNA and small oligonucleotides from AuNRs[18, 20, 21]; however, it was unclear whether the same principle could be extended to proteins that are very sensitive to temperature. Our results show that the selection of specific single strand DNAs (and thus melting temperature range) as well as spacer lengths between the oligonucleotide and the thiol group for AuNR, leads to the development of a system that is responsive to NIR light and has minimal[12] impact in the activity of the protein after release. Although the release of proteins from light-triggerable nanoformulations [12, 41] has been documented, this is the first report demonstrating the sequential release of more than one protein. In one study[12], the authors have conjugated a model protein (green fluorescent protein) with a histidine tag to a linker containing in one terminal a nickel chelator and in the other terminal a thiol group for the conjugation to a hollow gold nanoshell. The release of the protein was demonstrated after exposure to a NIR pulsed laser that melted the gold-thiol bonds. The authors have demonstrated the intracellular release of the protein but not its intracellular activity. Moreover, the formulation reported was not permissive to the release of more than one protein with an independent release profile. Another study described the intracellular delivery of a functional enzyme using upconversion nanoparticles conjugated with a spiropyran, a photoisomerizable compound[41]. After immobilization, spiropyran was irradiated with UV light to convert it into merocyanine form, which is positively charged at neutral pH and could be used to immobilize β-Gal through electrostatic interactions. NIR irradiation led to the emission of visible light by upconversion nanoparticles, converting merocyanine form to spiropyran and decreasing the electrostatic interaction with the protein, releasing β-Gal in its active form. Although the authors have demonstrated the intracellular delivery of proteins, the formulations reported were not permissive to the release of more than one protein with an independent release profile.

Conclusion

The current work reports a NIR light-activatable nanomaterial for the intracellular release of more than one protein, with independent release profiles. The novelty of the present work relies in the (i) development of an approach for the intracellular delivery of more than one active protein using NIR as a trigger, (ii) the demonstration that NIR light activates the release of the protein from the plasmonic carrier and the endolysosomal escape of both carrier and protein, and (iii) the demonstration of protein release from a carrier that has been accumulated within the cell between 4 h and at least 1 day (temporal control). The system documented here is based on the hybridization of a protein-modified with a single strand DNA (with a specific melting temperature) to a complementary single strand DNA immobilized on the surface of the AuNR. Upon NIR illumination at 780 nm, a photothermal effect occurs, leading to the melting of the double strand DNA and consequent release of the protein. We have demonstrated this principle for the controlled release of two proteins from the same carrier using a single NIR laser wavelength. The intracellular delivery of proteins has been demonstrated by microscopy localization studies, FRET acceptor photobleaching studies and enzyme intracellular activity measurements. Our results show that the NIR laser triggers the release of the protein from the AuNR and the escape of both AuNRs and protein from the endolysosomal compartment. Overall, the current work opens new possibilities for the design of materials to control the release of proteins, which may have implications in the areas of cellular reprogramming, cell modulation and gene editing.

Acknowledgements

The authors would like to thank the financial support of FCT (SFRH/BD/81705/2011 to ML; SFRH/BPD/105327/2014 to SS and SFRH/BPD/96048/2013 to SP) and EC (ERC project nº 307384, “Nanotrigger”).

References

1. B. Leader, Q. J. Baca and D. E. Golan, *Nat Rev Drug Discov*, 2008, **7**, 21-39.
2. Z. Gu, A. Biswas, M. Zhao and Y. Tang, *Chem Soc Rev*, 2011, **40**, 3638-3655.
3. N. W. S. Kam and H. Dai, *Journal of the American Chemical Society*, 2005, **127**, 6021-6026.
4. Y. Liu, H. Wang, K.-i. Kamei, M. Yan, K.-J. Chen, Q. Yuan, L. Shi, Y. Lu and H.-R. Tseng, *Angewandte Chemie International Edition*, 2011, **50**, 3058-3062.

5. J. Wu, N. Kamaly, J. Shi, L. Zhao, Z. Xiao, G. Hollett, R. John, S. Ray, X. Xu, X. Zhang, P. W. Kantoff and O. C. Farokhzad, *Angew Chem Int Ed Engl*, 2014, **53**, 8975-8979.
6. S. Zhu, L. Nih, S. T. Carmichael, Y. Lu and T. Segura, *Advanced Materials*, 2015, **27**, 3620-3625.
7. A. Erazo-Oliveras, K. Najjar, L. Dayani, T. Y. Wang, G. A. Johnson and J. P. Pellois, *Nat Methods*, 2014, **11**, 861-867.
8. P. Ghosh, X. Yang, R. Arvizo, Z.-J. Zhu, S. S. Agasti, Z. Mo and V. M. Rotello, *Journal of the American Chemical Society*, 2010, **132**, 2642-2645.
9. D. S. D'Astolfo, R. J. Pagliero, A. Pras, W. R. Karthaus, H. Clevers, V. Prasad, R. J. Lebbink, H. Rehmann and N. Geijsen, *Cell*, 2015, **161**, 674-690.
10. T. Graf and T. Enver, *Nature*, 2009, **462**, 587-594.
11. A. Y. Rwei, W. Wang and D. S. Kohane, *Nano Today*, 2015, **10**, 451-467.
12. D. P. Morales, G. B. Braun, A. Pallaoro, R. Chen, X. Huang, J. A. Zasadzinski and N. O. Reich, *Molecular Pharmaceutics*, 2015, **12**, 600-609.
13. R. Tong, H. D. Hemmati, R. Langer and D. S. Kohane, *Journal of the American Chemical Society*, 2012, **134**, 8848-8855.
14. A. A. Foster, C. T. Greco, M. D. Green, T. H. Epps and M. O. Sullivan, *Advanced Healthcare Materials*, 2015, **4**, 760-770.
15. S. Febvay, D. M. Marini, A. M. Belcher and D. E. Clapham, *Nano Letters*, 2010, **10**, 2211-2219.
16. A. E. Vasdekis, E. A. Scott, C. P. O'Neil, D. Psaltis and J. A. Hubbell, *ACS Nano*, 2012, **6**, 7850-7857.
17. J. Pérez-Juste, I. Pastoriza-Santos, L. M. Liz-Marzán and P. Mulvaney, *Coordination Chemistry Reviews*, 2005, **249**, 1870-1901.
18. R. Huschka, A. Barhoumi, Q. Liu, J. A. Roth, L. Ji and N. J. Halas, *ACS Nano*, 2012, **6**, 7681-7691.
19. F. Wang, Y. Shen, W. Zhang, M. Li, Y. Wang, D. Zhou and S. Guo, *Journal of Controlled Release*, 2014, **196**, 37-51.
20. S. E. Lee, G. L. Liu, F. Kim and L. P. Lee, *Nano Letters*, 2009, **9**, 562-570.
21. R. Huschka, J. Zuloaga, M. W. Knight, L. V. Brown, P. Nordlander and N. J. Halas, *Journal of the American Chemical Society*, 2011, **133**, 12247-12255.
22. Z. Jiang, H. Li, Y. You, X. Wu, S. Shao and Q. Gu, *Journal of Biomedical Materials Research Part A*, 2015, **103**, 65-70.
23. P. K. Jain, W. Qian and M. A. El-Sayed, *Journal of the American Chemical Society*, 2006, **128**, 2426-2433.
24. G. B. Braun, A. Pallaoro, G. Wu, D. Missirlis, J. A. Zasadzinski, M. Tirrell and N. O. Reich, *ACS Nano*, 2009, **3**, 2007-2015.
25. B. Nikoobakht and M. A. El-Sayed, *Chemistry of Materials*, 2003, **15**, 1957-1962.
26. A. Wijaya and K. Hamad-Schifferli, *Langmuir*, 2008, **24**, 9966-9969.
27. A. K. Kenworthy, *Methods*, 2001, **24**, 289-296.
28. K. W. Dunn, M. M. Kamocka and J. H. McDonald, *American Journal of Physiology - Cell Physiology*, 2011, **300**, C723-C742.
29. J. J. Storhoff, R. Elghanian, C. A. Mirkin and R. L. Letsinger, *Langmuir*, 2002, **18**, 6666-6670.
30. J. A. Díaz and J. M. Gibbs-Davis, *Small*, 2013, **9**, 2862-2871.
31. M. Ieda, J.-D. Fu, P. Delgado-Olguin, V. Vedantham, Y. Hayashi, B. G. Bruneau and D. Srivastava, *Cell*, 2010, **142**, 375-386.
32. C. S. Yun, A. Javier, T. Jennings, M. Fisher, S. Hira, S. Peterson, B. Hopkins, N. O. Reich and G. F. Strouse, *Journal of the American Chemical Society*, 2005, **127**, 3115-3119.
33. M. P. Singh and G. F. Strouse, *Journal of the American Chemical Society*, 2010, **132**, 9383-9391.
34. J. A. Brzostowski, T. Meckel, J. Hong, A. Chen and T. Jin, in *Current Protocols in Protein Science*, John Wiley & Sons, Inc., 2001, DOI: 10.1002/0471140864.ps1905s56.
35. M. Potokar, M. Stenovec, M. Gabrijel, L. Li, M. Kreft, S. Grilc, M. Pekny and R. Zorec, *Glia*, 2010, **58**, 1208-1219.
36. Y. Hu, T. Litwin, A. R. Nagaraja, B. Kwong, J. Katz, N. Watson and D. J. Irvine, *Nano Lett*, 2007, **7**, 3056-3064.
37. Ž. Krpetić, P. Nativo, V. Sée, I. A. Prior, M. Brust and M. Volk, *Nano Letters*, 2010, **10**, 4549-4554.
38. R. Vankayala, Y. K. Huang, P. Kalluru, C. S. Chiang and K. C. Hwang, *Small*, 2014, **10**, 1612-1622.
39. K. L. Levitsky, J. J. Toledo-Aral, J. López-Barneo and J. Villadiego, *Scientific Reports*, 2013, **3**, 2937.
40. J. R. Casey, S. Grinstein and J. Orlowski, *Nat Rev Mol Cell Biol*, 2010, **11**, 50-61.
41. L. Zhou, Z. Chen, K. Dong, M. Yin, J. Ren and X. Qu, *Advanced Materials*, 2014, **26**, 2424-2430.

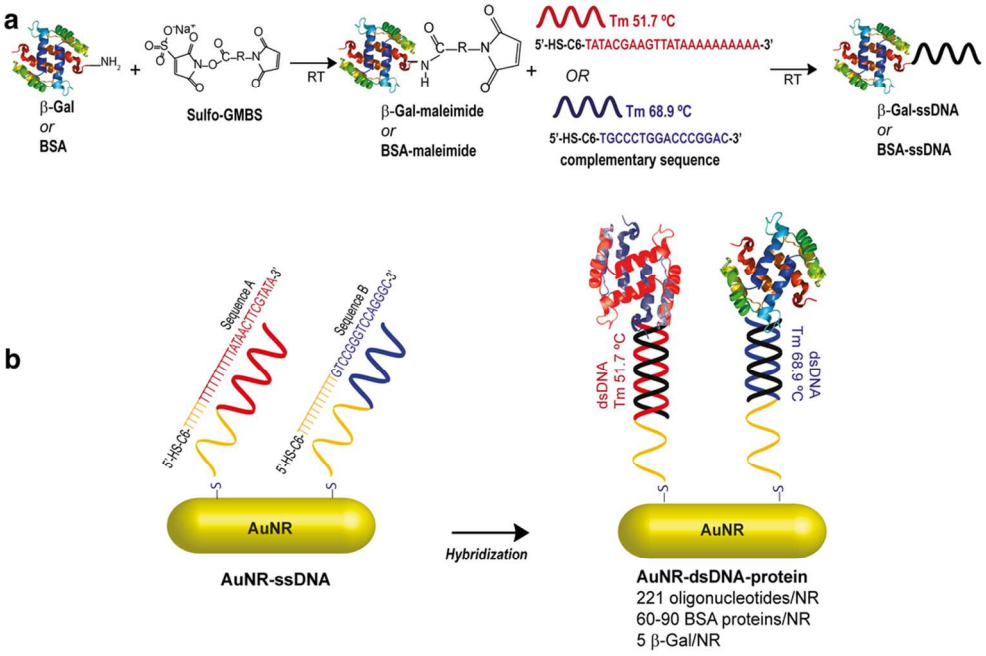

Figure. 1. Preparation of AuNR-DNA-protein conjugates. (a) Preparation of ssDNA-protein conjugates. Proteins (β-Gal or BSA) were initially reacted with a heterofunctional linker (Sulfo-GMBS) by its terminal succinimide ester. The protein conjugate was then reacted with a ssDNA having a terminal thiol group. After reaction, the protein conjugate (BSA-ssDNA or β-Gal-ssDNA) was purified by HPLC. (b) Preparation of AuNRssDNA. AuNRs were reacted with HS-ssDNA complementary to the strands of BSA-ssDNA or β-Gal-ssDNA conjugates. The ssDNA-protein conjugates were then bound to the ssDNA-AuNR by hybridization. Upon NIR irradiation, there is an increase in the temperature at the AuNR leading to the DNA de-hybridization and the release of proteins with different kinetics. The release kinetic depends on the heat generated (which depends on the power of NIR laser used) and the melting temperature of the oligonucleotides.

101x67mm (300 x 300 DPI)

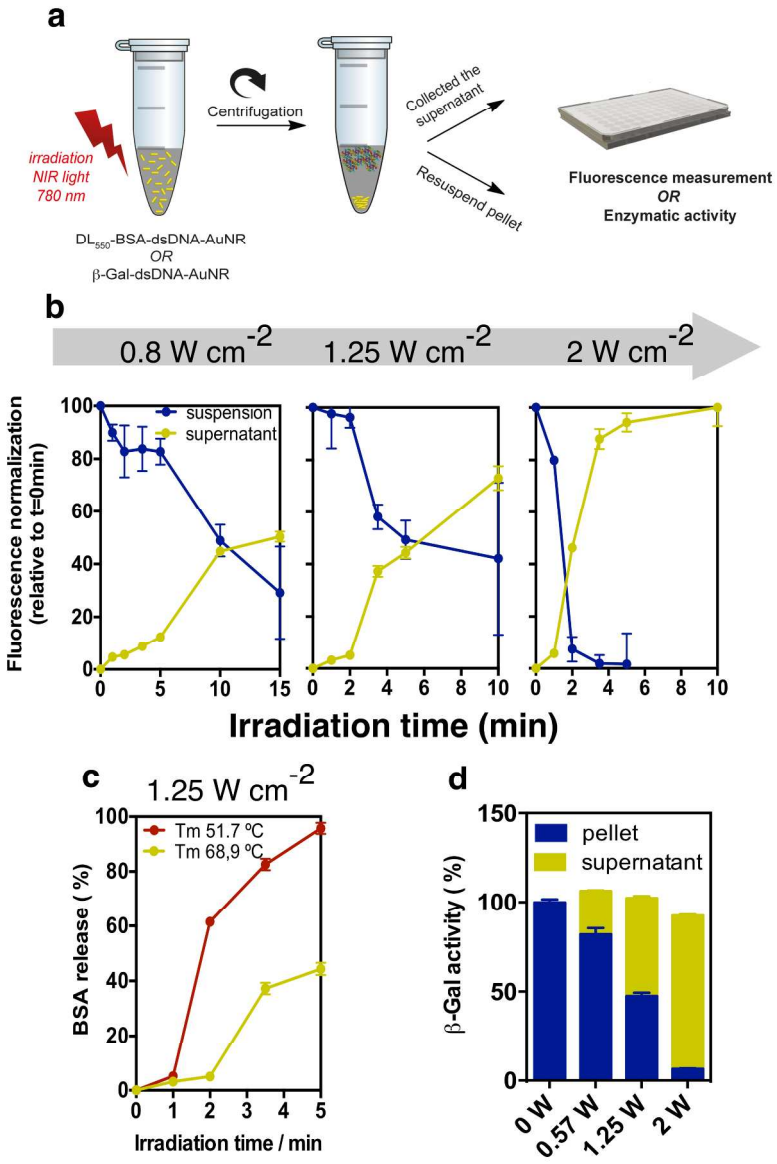

Figure 2. In vitro release of BSA-ssDNA or β-Gal-ssDNA from AuNRs conjugated with complementary ssDNA. (a) Schematic representation of the in vitro release experiments. Fluorescently-labeled-protein-dsDNA-AuNR were irradiated by a NIR laser (780 nm) up to 15 min after which the suspension was centrifuged and the protein fluorescence (BSA) or the enzyme activity (β-Gal) measured both in the supernatant and pellet. (b) Release profile of BSA from DL550-BSA-dsDNA68.9-AuNR irradiated with different NIR laser powers up to 15 min. (c) Release profiles of BSA from DL550-BSA-dsDNA68.9-AuNR or DL488-BSA-dsDNA51.7-AuNR, irradiated with a NIR laser (780 nm; laser power: 1.25 W cm-2) up to 5 min. (d) Relative β-Gal activity in the supernatant and in the pellet after release from β-Gal-dsDNA51.7-AuNR. Each β-Gal activity after laser irradiation was normalized by the total enzyme activity before laser irradiation. In b, c and d, results are Average ± SD (n=3).

127x195mm (600 x 600 DPI)

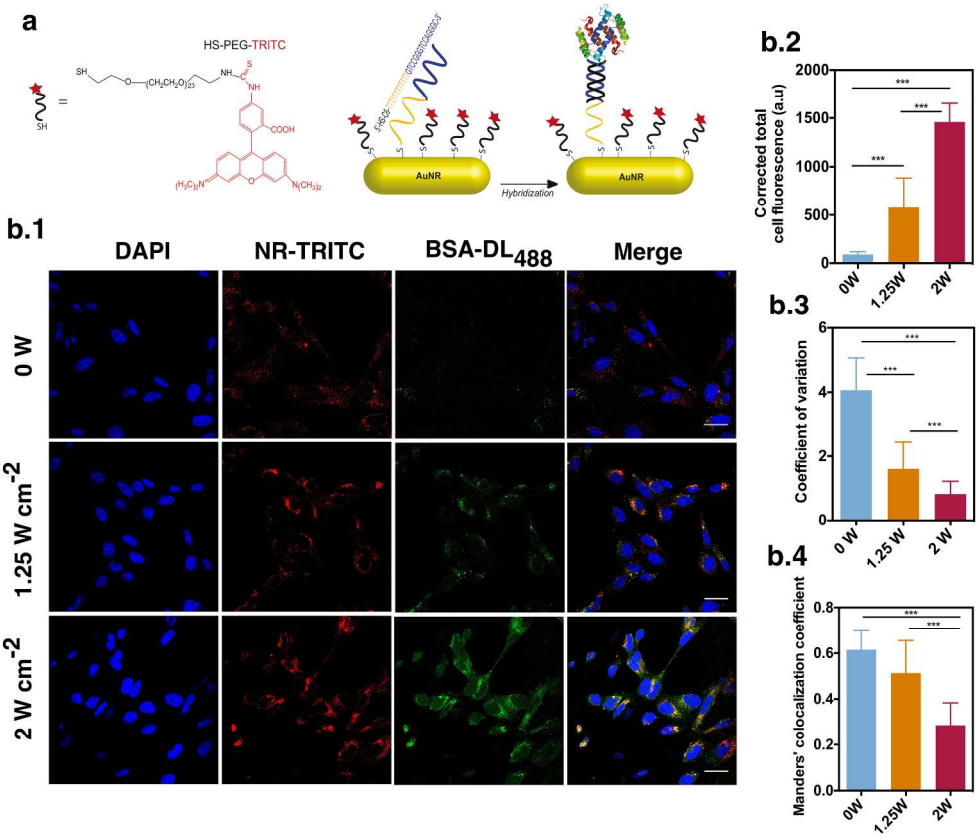

Figure 3. Intracellular release of proteins. Fibroblasts were incubated with DL488-BSA-dsDNA68.9-AuNR-TRITC for 4 h, washed, new cell culture media added and finally irradiated with a laser at 780 nm (laser power: 1.25 or 2 W cm-2) for 2 min. (a) Schematic representation for the preparation of DL488-BSA-dsDNA68.9-AuNR-TRITC. The stoichiometry between ssDNA and TRITC is 1:4.5. (b.1) Representative confocal images of fibroblasts after incubation with DL488-BSA-dsDNA68.9-AuNR with and without laser irradiation. Scale bar is 30 μm. (b.2 and b.3) Intensity and coefficient of variation of the signal of DL488-BSA-ssDNA68.9. (b.4) Colocalization between AuNR-TRITC and DL488-BSA-ssDNA68.9 expressed as Manders' overlap coefficient assessed by ImageJ analysis. In b.2-b.4, the results are expressed as Average ± SD (n=3). *** denotes statistical significance ($p<0.001$) assessed by one-way ANOVA followed by Tukey's post-hoc test.

127x108mm (600 x 600 DPI)

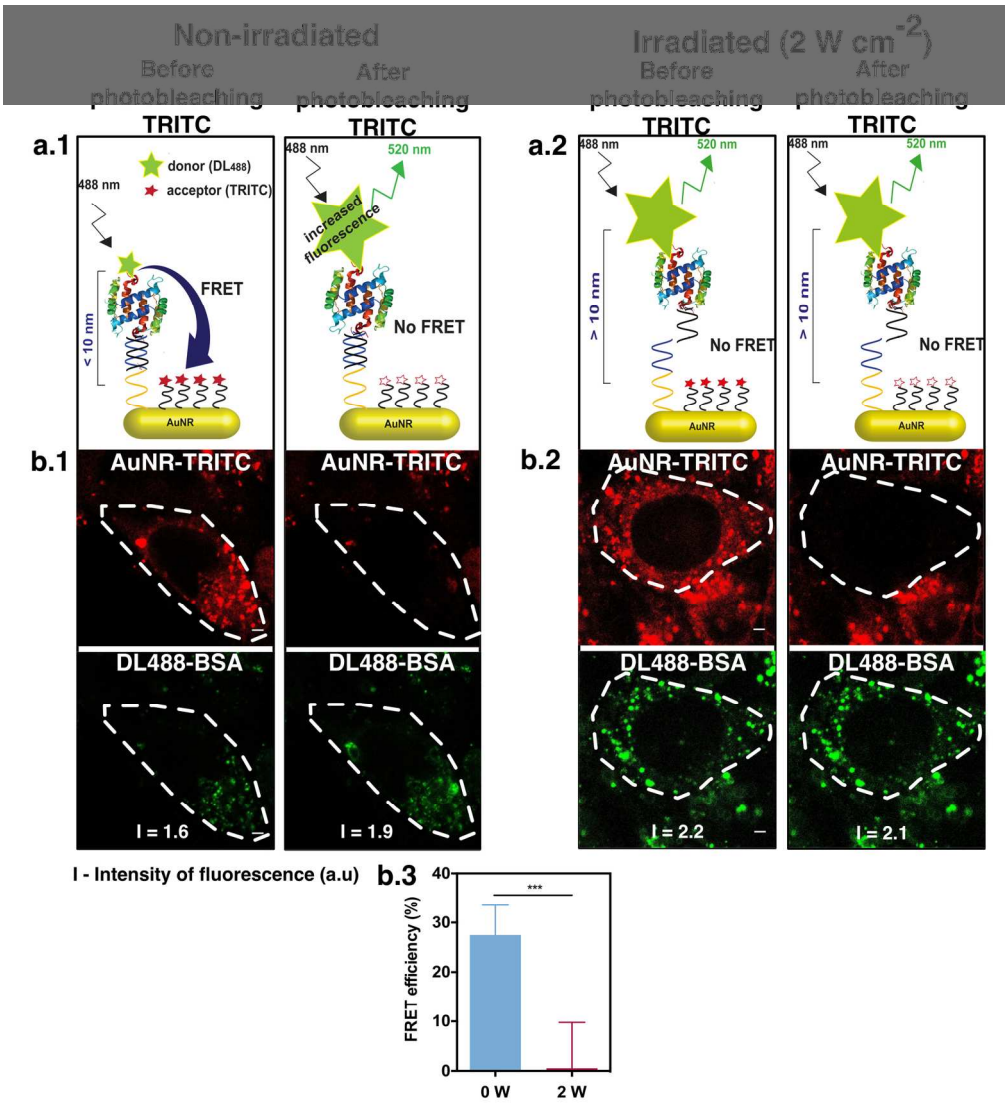

Figure 4. FRET analysis to evaluate the proximity of the protein to the AuNR-TRITC. (a.1 and a.2) Schematic representation of the acceptor photobleaching FRET method. DL488 works as donor, transferring energy to the acceptor (TRITC). If the distance between the pair is less than 10 nm, when the acceptor is photobleached, the fluorescence of the donor increases. (b) Fibroblasts were incubated with DL488-BSAdsDNA68.9-AuNR-TRITC (50 μg mL-1) for 4 h, washed, feeded with new cell culture media, and either irradiated or not with a 780 nm laser for 2 min (2 W cm-2). (b.1 and b.2) Confocal images of AuNR-TRITC and DL488-BSA-ssDNA68.9 before and after photobleaching TRITC within a region of interest (ROI, each ROI corresponds to one cell) with confocal 561 nm laser (80% of intensity). Scale bar is 6 μm. (b.3) Quantification of FRET efficiency. FRET efficiency (FRETeff) was calculated as FRETeff = ([Dafter]-[Dbefore])/[Dafter])x100, where Dafter is the fluorescence intensity of the donor (DL488) after photobleaching of the acceptor (TRITC), and Dbefore is the fluorescence intensity of the donor before photobleaching of the acceptor. Results are Average ± SD (n=10 cells, ***p < 0.001).

165x181mm (300 x 300 DPI)

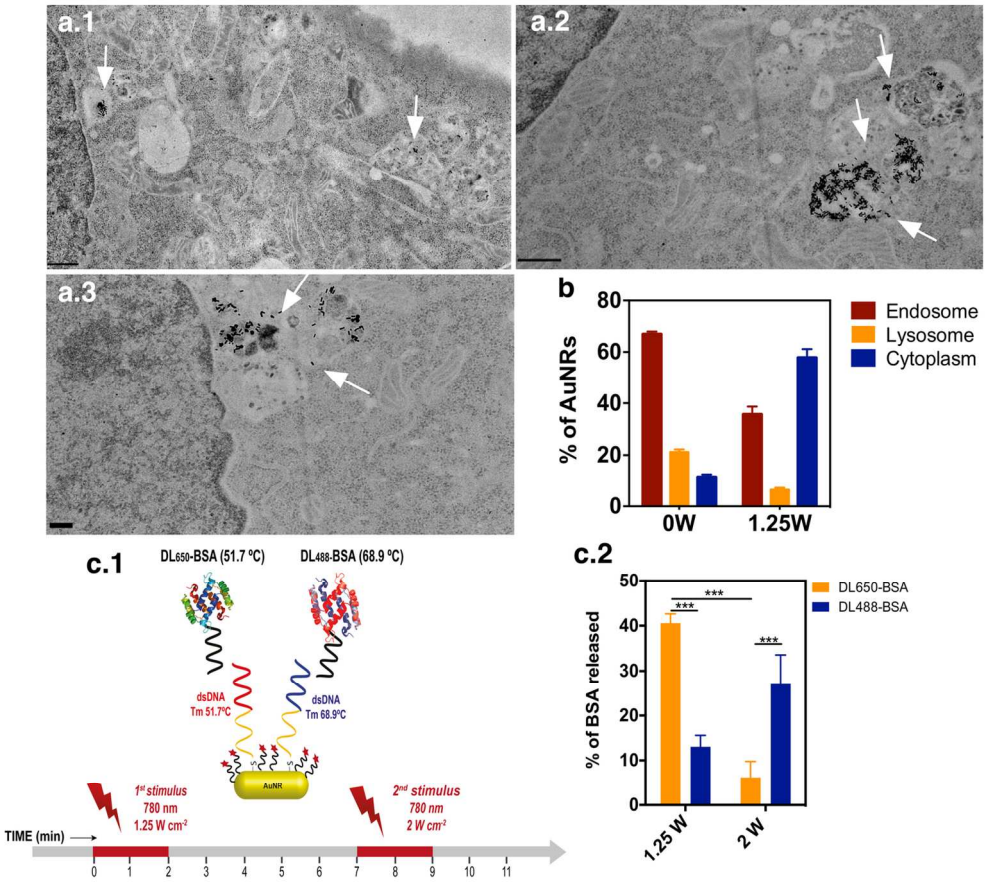

Figure 5. Laser induced endosomal escape. (a) TEM images of fibroblasts incubated with BSA-dsDNA51.7-uNR for 4 h before (a.1) and after (a.2 and (a.3) laser irradiation (2 min at 1.25 W cm-2). In a.1, white arrows indicate the presence of AuNR accumulated in vesicles. Figures a.2 and a.3 are representative TEM images of endosomal damage induced by laser irradiation with rupture of the endosomal membrane and consequent escape of the AuNR to the cytoplasm. In a.1, a.2 and a.3, N means cell nuclei. Scale bar is 500 nm in a.1 and a.2 and 200 nm in a.3. (b) Quantification of the amount of AuNR present in the cytoplasm and vesicles (endosomes and lysosomes). The percentage of AuNRs in each cell compartment was calculated after counting all the AuNRs accumulated within the cell. Results are Average ± SD (n = 30 images of amplification between 20000X and 80000X for 0 W and n = 20 images of amplification between 20000X and 80000X for 1.25 W) (c.1 and c.2) Intracellular delivery of two proteins. (c.1) Scheme illustrating the sequential release of two proteins from AuNRs in cells. Fibroblasts were incubated with AuNR-TRITC conjugated with DL650-BSA-dsDNA51.7 and DL488-BSA-dsDNA68.9 for 4 h. The cells were then washed with cell culture media and irradiated for 2 min at 1.25 W cm-2. A subset of samples was fixed with 4% PFA after irradiation and the other group was incubated for additional 5 min before being irradiated for 2 min at 2 W cm-2 and fixed afterwards. (c.2) The amount of protein released was calculated as %BSAR= 100 x (MCbefore - MCafter)/MCbefore, where MCbefore is the Manders' colocalization coefficient before irradiation and MCafter is the Manders' colocalization coefficient after irradiation. Results are Average ± SEM, n=3 (3 samples, 5 microscope fields per sample). Unpaired t-test was used to compare each condition (p value ≤ 0.0001).

135x122mm (300 x 300 DPI)

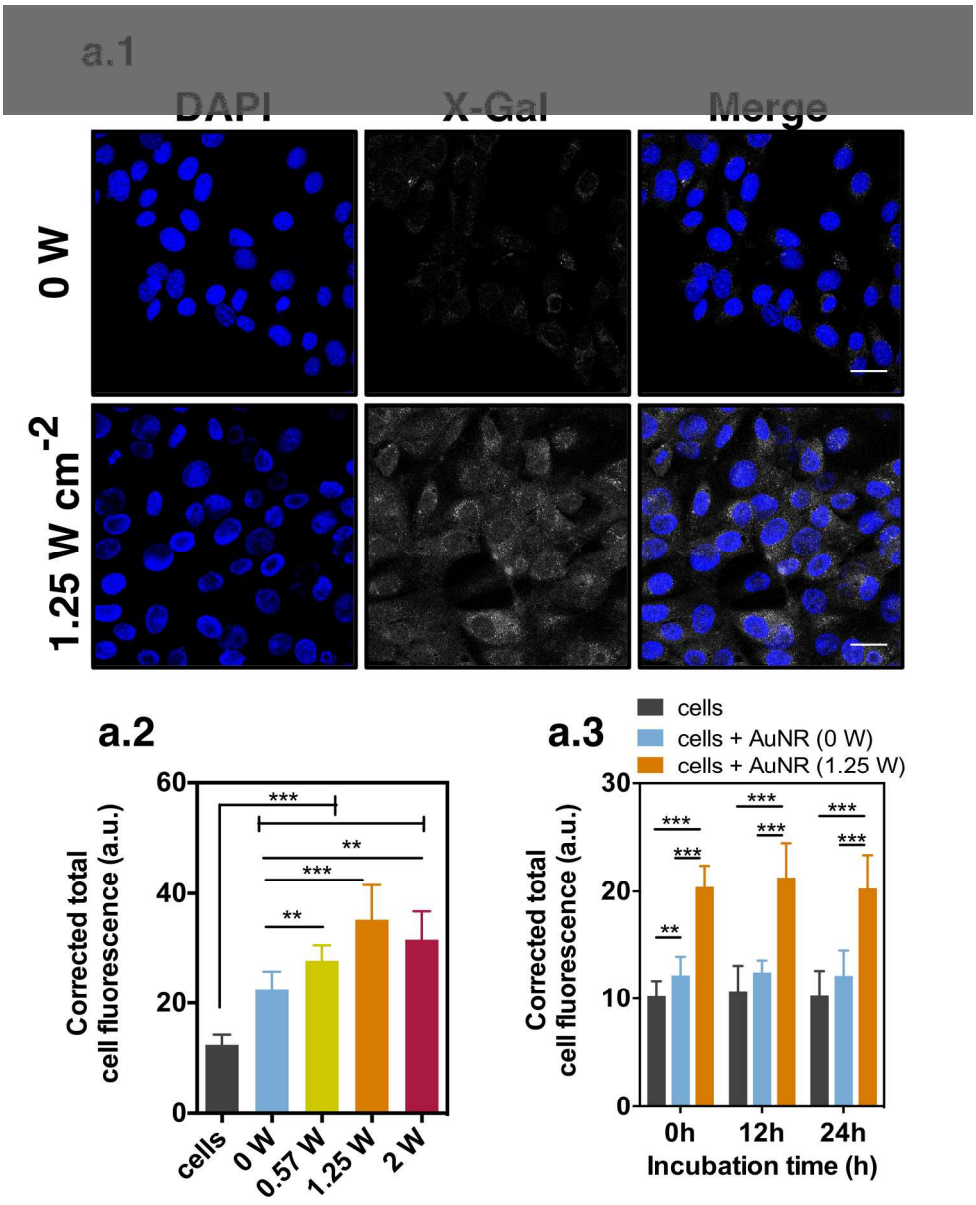

Figure 6. Intracellular activity of a protein released from AuNR-dsDNA51.7-βGal. Fibroblasts were incubated with AuNR-dsDNA51.7-βGal (50 μg mL-1) for 4 h, after which were washed, new culture media was added, and then were irradiated for 2 min (wavelength: 780 nm; laser powers: 0.57, 1.25 and 2 W cm-2). Then, the cells were immediately fixed and exposed to a β-Gal substrate (X-Gal) followed by confocal microscopy evaluation. (a.1) Representative confocal microscopy images. Scale bar is 30 μm. (a.2) Quantification of β-Gal activity. Cell fluorescence in each experimental condition was corrected to the corresponding background fluorescence and thus named as corrected total cell fluorescence. The group "cells" means cells without AuNRs. Results are expressed as Average ± SD, n=3 (3 samples, 5 microscope fields per sample). (a.3) Quantification β-Gal activity. After 4 h incubation, medium was replaced and cells were irradiated immediately (0 h), 12 h or 24 h after. In a.2 and a.3, results are expressed as Average ± SD, n=3 (3 samples, 5 microscope fields per sample). **, *** denote statistical significance ($p<0.01$; $p<0.001$) assessed by one-way ANOVA followed by a Tukey's post-hoc test.

Intracellular delivery of more than one protein with spatio-temporal control

Miguel M. Lino, Susana Simões, Sónia Pinho and Lino Ferreira.*

CNC, Center for Neurosciences and Cell Biology and Faculty of Medicine, Polo III - Health Sciences Campus University of Coimbra, Rua Larga, 3004-517, Coimbra, Portugal

Supporting Information

Experimental Section

Materials. β-Galactosidase (β-Gal) from *Escherichia coli*, thiolated oligonucleotide strands, hexadecyltrimethylammonium bromide (CTAB), sodium borohydride ($NaBH_4$), silver nitrate ($AgNO_3$), hexanethiol and mercaptohexanoic acid, and other chemicals were all purchased from Sigma-Aldrich and used as received without further purification. Sodium dodecyl sulfate (SDS) was purchased from VWR. Bovine Serum Albumin (BSA), DyLight-NHS ester, N-[γ-maleimidobutyryloxy] sulfosuccinimide ester (sulfo-GMBS), LysoTracker® Green DND-26, LysoTracker® Red DND-99, fetal bovine serum (FBS) and trypsin-EDTA solution were purchased from Thermo Fisher Scientific. Dulbecco's Modified Essential Medium (DMEM) is a commercial product of Merck Millipore. Purified

water with resistivity above 18.2 $M\Omega.cm^{-1}$ was obtained by reverse osmosis (MilliQ, Millipore). Other reagents were analytical grade.

Characterization of protein conjugated with ssDNA by non-denaturing PAGE. The reaction mixture obtained after reacting the proteins with ssDNA and the fractions obtained after HPLC purification of the reaction mixture were analysed by gel electrophoresis. Reaction mixture (15 µL) and reaction mixture fractions obtained after HPLC purification (15 µL) were mixed with glycerol (5 µL; glycerol in 50% v/v of H_2O), loaded in a polyacrylamide gel (12%, w/v) and run for 45 min in 0.5 x TBE at 140 V. The gel was stained with SyBr Gold (1:5000 in 1 x TBE) for 10 min and imaged in a UV transilluminator (Molecular Imager Gel DOC, Biorad).

Uptake kinetics of βGal-dsDNA-AuNR. SC-1 cells were plated in a 24 well plate at a density of $5x10^4$ cells/well and left to adhere overnight. The cells were incubated with βGal-dsDNA-AuNR (50 µg mL^{-1}) for 1, 2, 4, 6 and 24h. After incubation, in order to remove non-internalized nanorods, the cells were washed three times with PBS, dissociated with trypsin and counted. Finally, the samples were freeze-dried and the amount of gold was determined by inductive coupled plasma mass spectrometry (ICP-MS). In order to evaluate the levels of internalized AuNRs along the time, cells were incubated with βGal-dsDNA-AuNR for 4 h and after washing three times with PBS, cells were left in the incubator for 3, 6, 12 or 24 h. In a subset of samples, after incubation with βGal-dsDNA-AuNR, cells were treated with Mitomycin C (8 µg mL^{-1}, Sigma) for 2h30, to inhibit cell proliferation.

Cytotoxicity of BSA-dsDNA-AuNR. To assess the cytotoxicity of AuNRs, SC-1 fibroblasts were seeded on a 96 well plate (4 x 10^3 cells/well), left to adhere for 24 h and then incubated with BSA-dsDNA51.7-AuNR (concentrations between 10 and 200 µg mL^{-1}) for 4 h. After incubation, cells were

washed with medium to remove non-internalized AuNRs. In some conditions, after incubation with BSA-dsDNA-AuNR, cells were washed and irradiated with a fibercoupled Roithner laser (780 nm). Each well was placed below the end of the fibre and irradiated with a power density of 1.25 or 2 W cm^{-2} for 2 min. Then cells were left in the incubator for 24 h and the ATP production was measured by a Celltiter-Glo Luminescent Cell Viability Assay (Promega).

In a separate experiment, the cytotoxicity of AuNRs was evaluated by an Annexin/PI assay. Cells were seeded in a 48 well plate (20000 cells/well), left to adhere for 24 h and incubated with BSA-dsDNA51.7-AuNR at 20, 50 and 100 μg mL^{-1}, for 4 h. After washing to remove non-internalized AuNRs, cells were irradiated at 1.25 or 2 W cm^{-2} for 2 min. After 24 h incubation at 37 ºC, the medium containing detached cells was collected and the adherent cells were rinsed with PBS and trypsinized. After centrifuging, the pellet was resuspended in 100 μL of binding buffer containing 2.5 μL of Annexin V-FITC conjugate (Invitrogen). After 15 min incubation, 100 μL of propidium iodide (2 μg mL^{-1}) were added to each tube and then the cells were kept on ice until analysis by flow cytometry.

Immunocytochemistry. Cells were seeded in gelatin coated coverslips and left to adhere for 24 h. After 4h incubation with βGal-dsDNA-AuNR (50 μg mL^{-1}), cells were irradiated with 780 nm laser at 1.25 W cm^{-2}. The samples were immediately fixed after irradiation with paraformaldehyde 4% (v/v) for 15 min at room temperature followed by the washing (3 times) with PBS. After blocking (PBS solution with 1% BSA), cells were incubated with a rabbit anti-β-galactosidase antibody (Invitrogen) for 60 min, washed three times with blocking buffer and incubated with alexa-fluor488 conjugated goat anti-rabbit IgG (dilution 1:1000) for 60 min. The excess of antibody was removed by washing with PBS before staining with DAPI (1 μg mL^{-1}) for 5 min. Coverslips were analyzed in a confocal microscope (LSM 710, Carl Zeiss). The corrected total cell fluorescence was quantified with ImageJ and corrected for background fluorescence. Manders' colocalization coefficient was calculated using Image J and JACoP plugin.

Intracellular localization of AuNR-TRITC. Cells were seeded in an IBIDI 15 well slide (5000 cells/well), left to adhere for 24 h and then incubated with BSA-dsDNA-AuNR-TRITC (50 μg mL^{-1}) for 4 h. After incubation, cells were washed with medium to remove non-internalized AuNRs. Then, the cells were incubated with LysoTracker® Green (100 nM) for 30 min to stain the endosomes and with Hoechst 33342 (1μg mL^{-1}) to stain the nuclei. Cells were observed under confocal microscope, immediately after laser irradiation at 780 nm (1.25 and 2 Wcm^{-2}). The images were analyzed in ImageJ and the colocalization was determined by calculating the Manders' colocalization coefficient between AuNR-TRITC and Lysotracker green.

Light-induced endosomal escape. To study endosomal escape, cells were incubated with BSA-dsDNA-AuNR in the presence of a membrane impermeable molecule, calcein. Briefly, 5000 cells/well in a IBIDI slide were incubated with 50 μg mL^{-1} of BSA-dsDNA-AuNR and 0.25 mM calcein for 4h. After removing AuNRs, cells were incubated with lysotracker red (100 nM) for 30 min. Then, medium was replaced and cells were irradiated with 780 nm laser for 2 min (1.25 and 2 Wcm^{-2}) and analyzed under confocal microscope.

Supplementary Data

Supplementary table 1. Oligonucleotide strands used for the conjugation to AuNRs and for protein modification. The melting temperature refers to a theoretical melting temperature relative to the portion of the strand that is able to hybridize with the complementary strand.

	Tm / ºC	sequence
AuNR conjugation	51.7	5'-HS-C6-TTTTTTTTTTTTTTTATAACTTCGTATA-3'
	68.9	5'-HS-C6-TTTTTTTTTTTTGTCCGGGTCCAGGGC-3'
DNA-protein conjugates	51.7	5'-HS-C6-TATACGAAGTTATAAAAAAAAAA-3'
	68.9	5'-HS-C6-TGCCCTGGACCCGGAC-3'

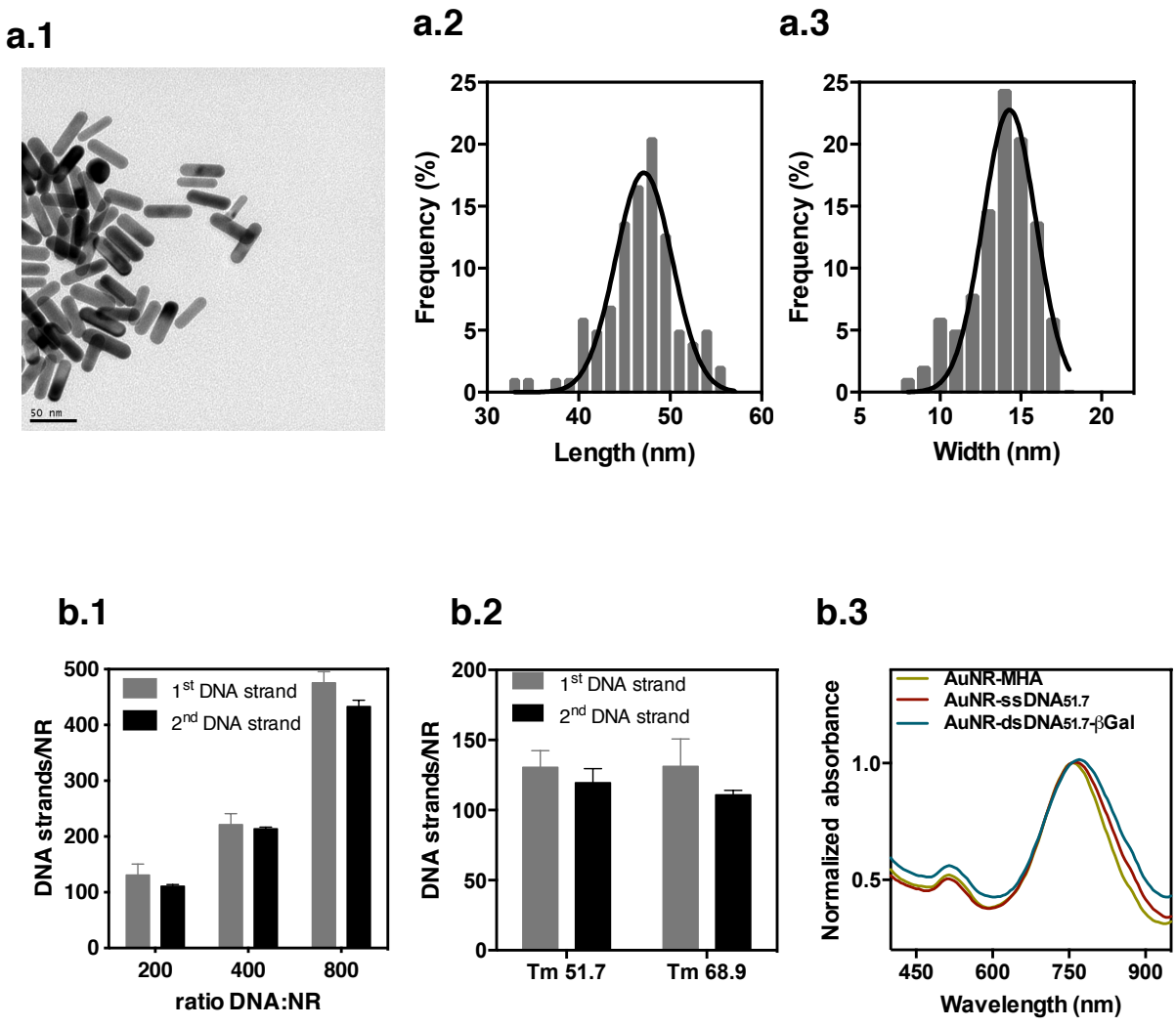

Figure S1. Characterization of AuNRs. (a) TEM analysis. (a.1) Representative TEM image of AuNRs. (a. 2-a.3) NR length (a.2) and width (a.3) distribution obtained from TEM images. The AuNRs showed an average length of 46.7 ± 4.1 nm, n=100 AuNRs and an average width of 13.8 ± 1.9 nm, n=100 AuNRs. (b.1) Quantification of oligonucleotides immobilized on NR surface via thiol gold chemistry (1st DNA strand) or hybridized to the ssDNA conjugated to the NR (2nd DNA strand). The amount of strands per AuNR was determined indirectly in the supernatant by measuring absorbance at 260 nm in Nanodrop. (b. 2) Comparison of the binding efficiency of the two sequences with different melting temperatures (91.7% efficiency for DNA strand with Tm 51.7 ºC and 84.5% efficiency for DNA strand with Tm 68.9 ºC). Results in b.1 and b.2 are Average ± SD, n=3. (b.3) Absorbance spectra of AuNRs after conjugation with mercaptohexanoic acid (AuNR-MHA); after conjugation with ssDNA51.7 (AuNR-ssDNA51.7) and after hybridization with β-Gal (AuNR-dsDNA51.7-βGal). Surface plasmon resonance band does not change significantly during surface modification.

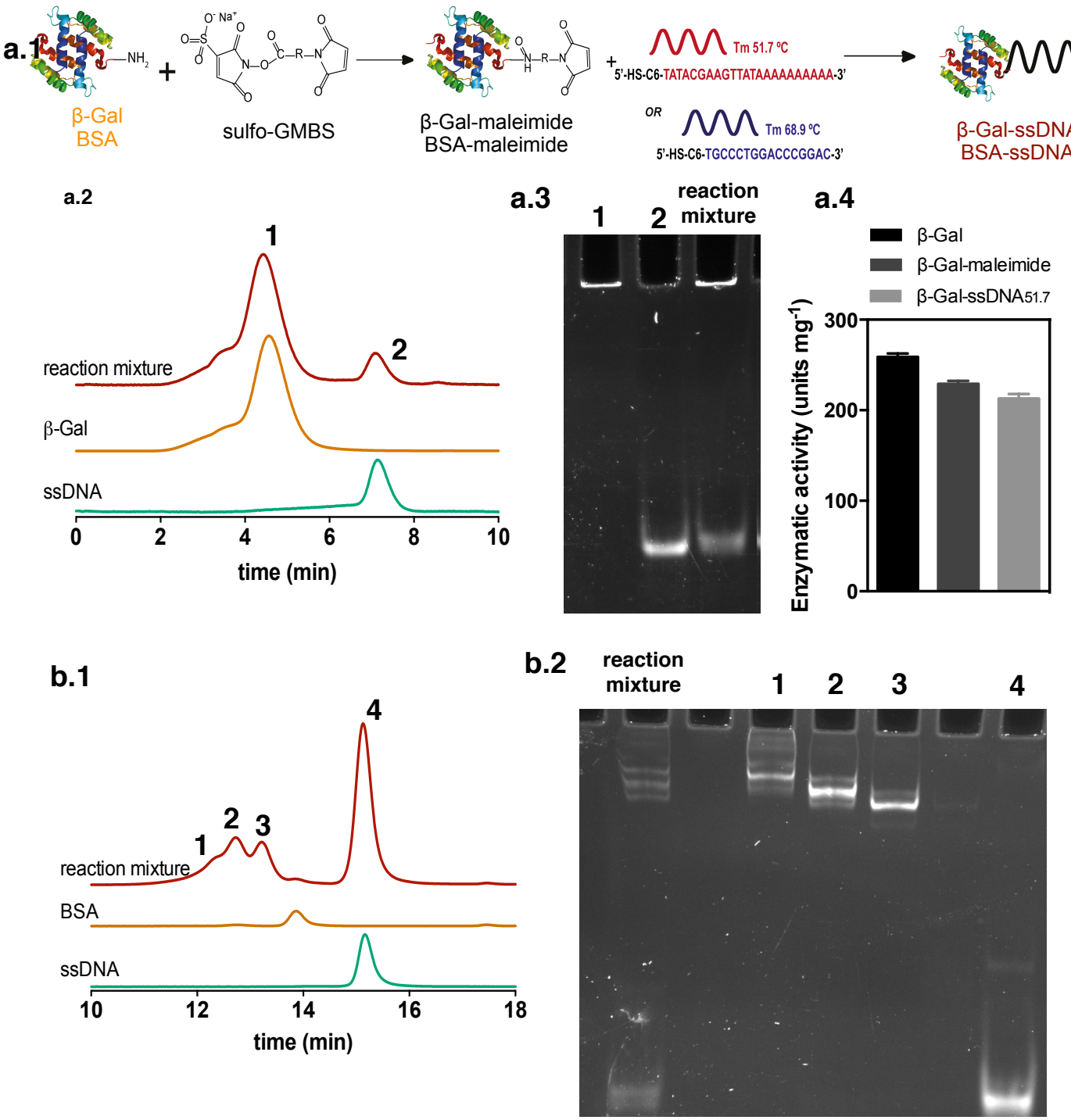

Figure S2. Characterization of oligonucleotide-protein conjugates. (a.1) Scheme showing the coupling reaction of ssDNA to the proteins. (a.2) HPLC characterization of the reaction mixture between β-Gal and ssDNA. Representative chromatograms of β-Gal, ssDNA and the final reaction mixture of β-Gal with ssDNA. Integration of DNA peaks indicate a conjugation value of 37% of the total DNA. This means that each protein molecule was conjugated with at least one oligonucleotide. (a.3) Electrophoresis characterization of the HPLC fractions. Fractions 1 and 2 were analysed. Samples were run in polyacrylamide gel and DNA (and not protein) was stained with Sybr Gold. Quantification of free DNA indicates a conjugation value of 35% of the total DNA. Fraction 1, which corresponds to the β-Gal-ssDNA conjugate was used for subsequent experiments. (a.4) Enzymatic activity β-Gal, β-Gal conjugated with sulfo-GMBS (β-Gal-maleimide) and β-Gal conjugated with ssDNA51.7 (β-Gal-ssDNA51.7). (b.1) HPLC characterization of the reaction mixture between BSA and ssDNA51.7. Representative chromatograms of BSA, ssDNA and the final reaction mixture of BSA with ssDNA. (b. 2) Electrophoresis characterization of the HPLC fractions. Fractions 1-4 were analyzed. Fraction 3 was used for conjugation with AuNR-ssDNA. We selected this fraction because each protein is conjugated with one ssDNA.

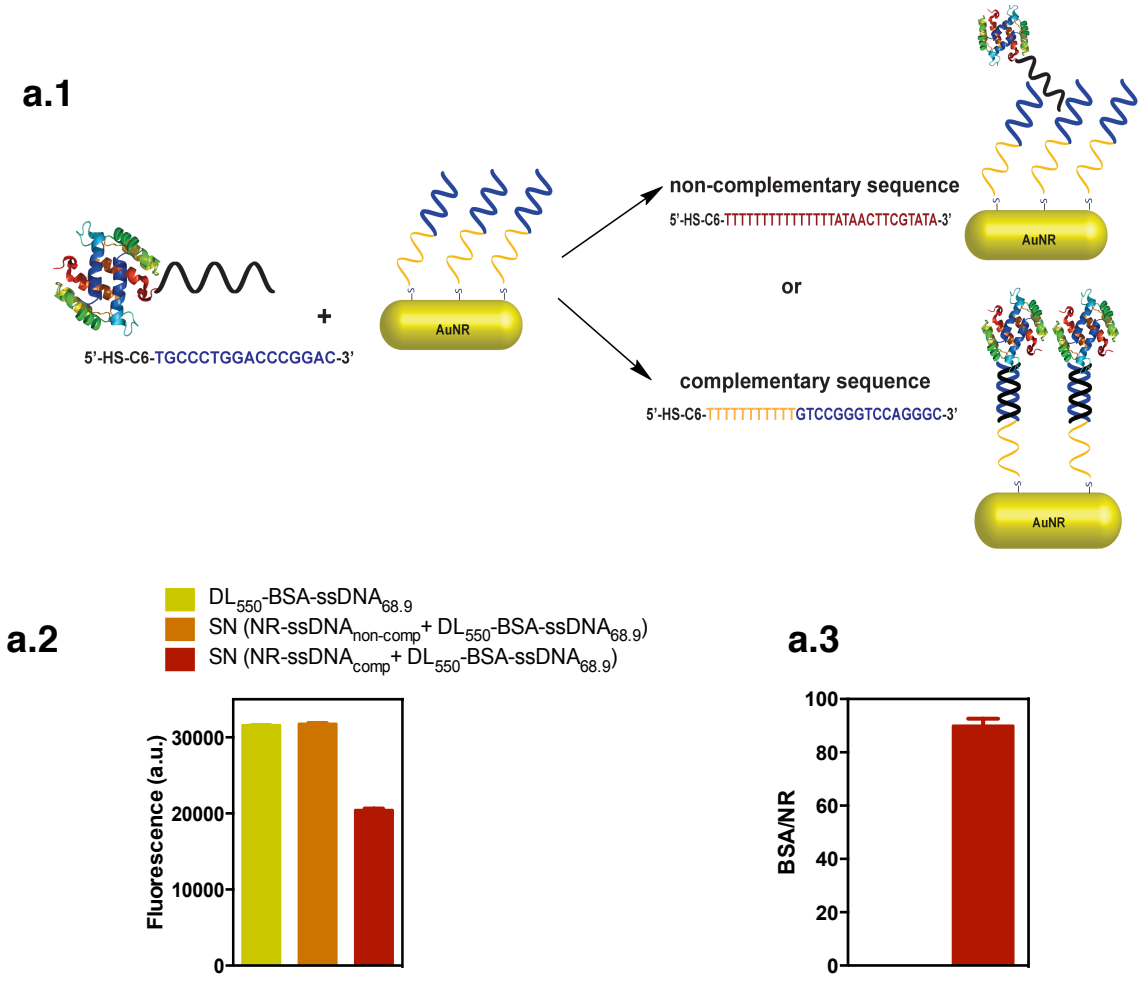

Figure S3. Specificity for the hybridization between AuNR-ssDNA and BSA-ssDNA. (a.1) Scheme showing the experiment set-up to demonstrate that the hybridization between AuNR-ssDNA68.9 and BSA-ssDNA68.9 was specific. (a.2) Fluorescence intensity of the supernatants collected after the hybridization of DL550-BSA-ssDNA68.9 to AuNRs conjugated with complementary (ssDNAcomp) or non-complementary (ssDNAnon-comp) oligonucleotide sequences. The ratio BSA to AuNRs was 1:300. DL550-BSA-ssDNA68.9 solution for hybridization was used as a control. (a.3) Number of proteins immobilised per AuNR, calculated indirectly from the fluorescence in the supernatant through a calibration curve (concentration between 2.5 and 50 nM, excitation at 480 nm and emission at 515 nm). In a.2 and a.3, results are Average ± SD, n=3.

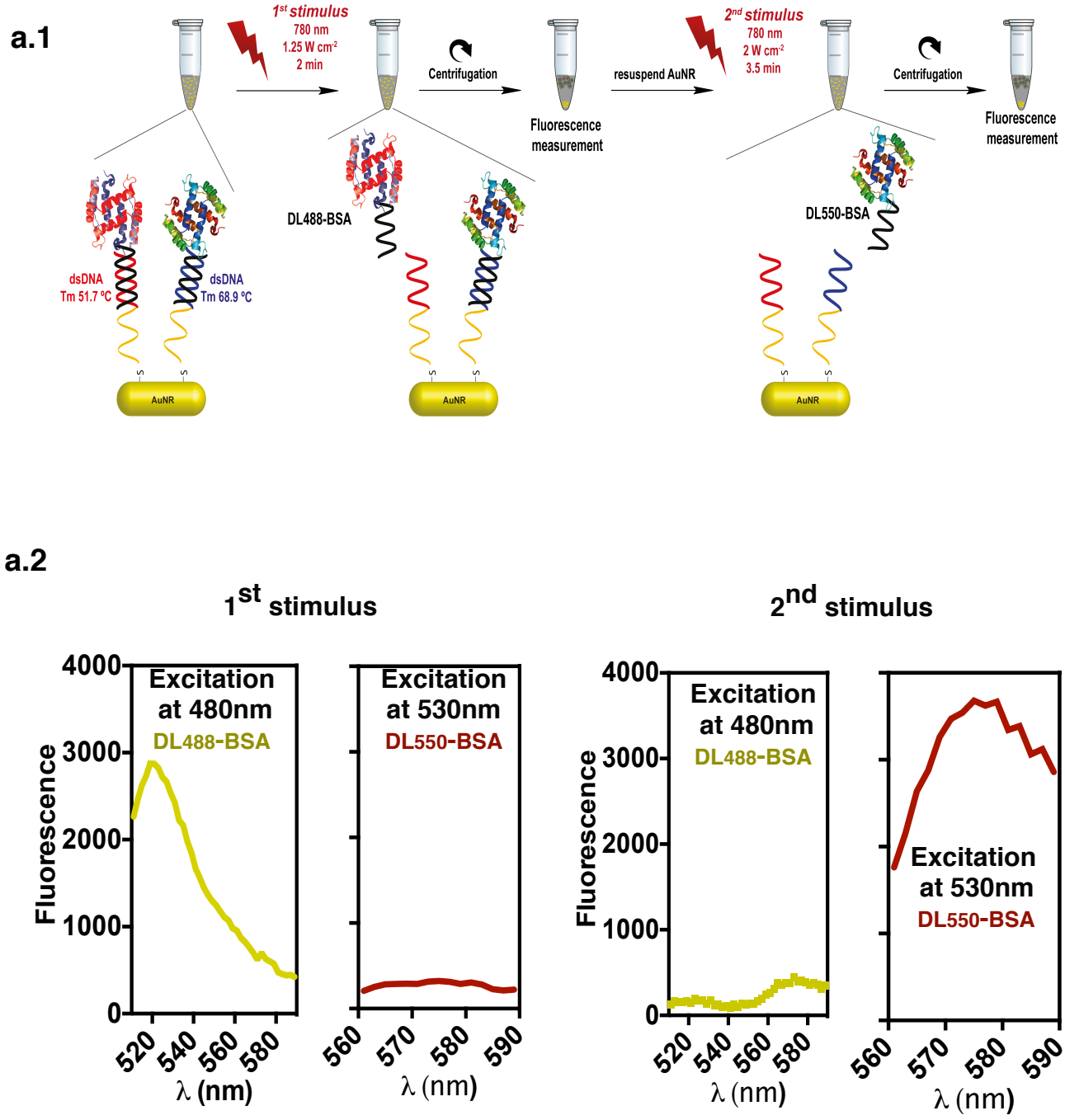

Figure S4. Sequential release of DL488-BSA-ssDNA51.7 and DL550-BSA-ssDNA68.9 from AuNRs after light activation. (a.1) Scheme illustrating dual release experiment. A suspension of DL488-BSA-dsDNA51.7-AuNR-DL550-BSA-dsDNA68.9 was first irradiated for 2 min at 1.25 W cm^{-2} and then centrifuged in order to collect the supernatant. The NR were resuspended and irradiated again at 2 W cm^{-2} for 3.5 min and then centrifuged. AuNRs used in this experiment were conjugated with 32 molecules of DL488-BSA-ssDNA51.7 and 34 molecules of DL550-BSA-ssDNA68.9. (a.2) The fluorescence of both supernatants was measured in a fluorimeter using an excitation wavelength at 480 nm for DL488-BSA or 530 nm for DL550-BSA. The first stimulus caused the release of 86% of DL488-BSA and 7% of DL550-BSA. The second stimulus released 14% of DL488-BSA and 93% of DL550-BSA.

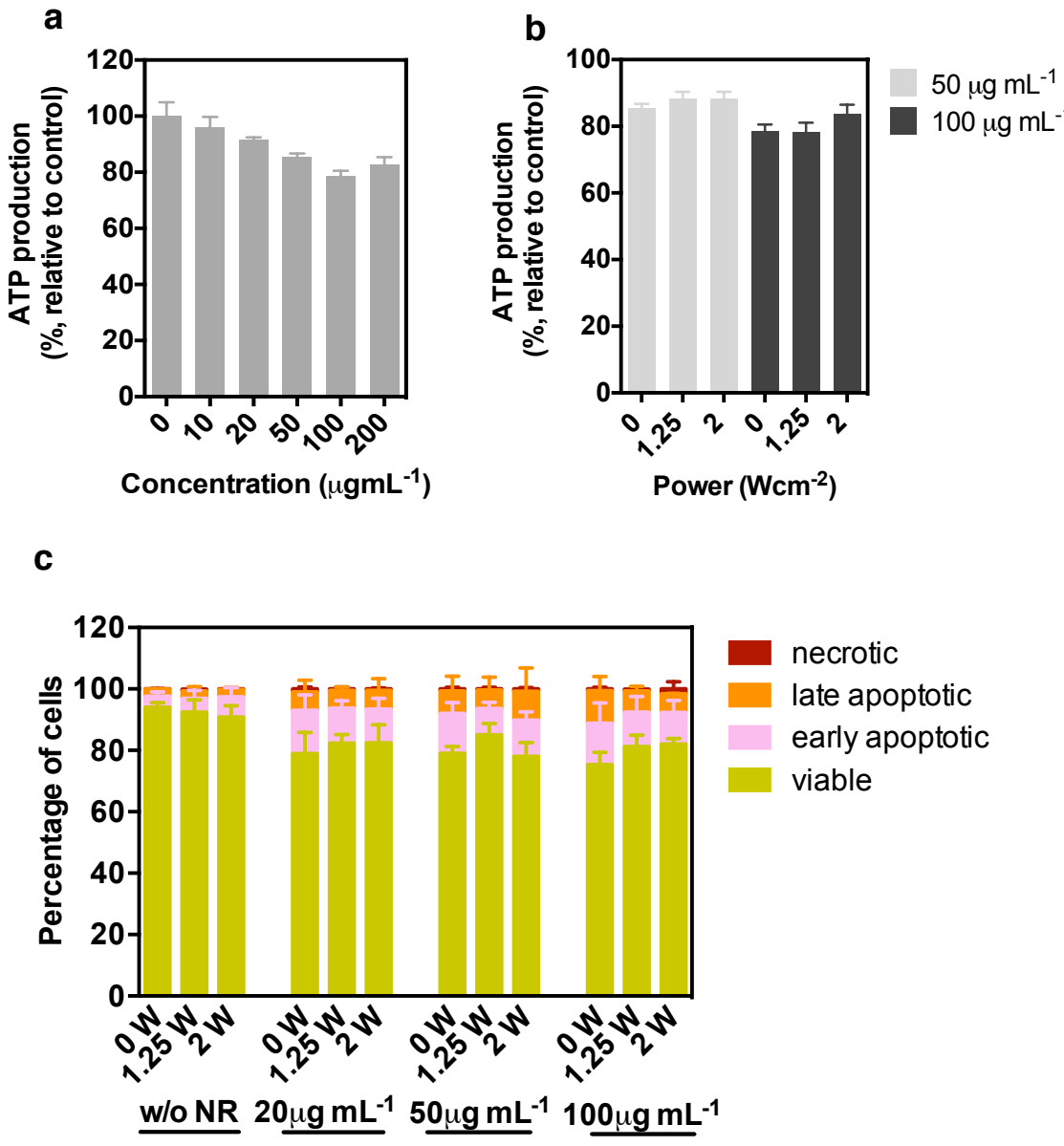

Figure S5. Cytotoxicity of BSA-dsDNA51.7-AuNR. Fibroblasts were incubated with different concentrations of BSA-dsDNA51.7-AuNR for 4 h, washed, incubated in cell culture media for 20 h after which cell metabolism (a and b) or cell viability (c) was evaluated by an ATP (a and b) or annexin V/PI (c) assays. Control are cells cultured without AuNRs. (a and b) Cytotoxicity of non-irradiated BSA-dsDNA51.7-AuNR (a) and irradiated BSA-dsDNA51.7-AuNR (780 nm laser for 2 min; laser powers: 1.25 and 2 W cm^{-2}) (b) as evaluated by an ATP assay. (c) Cytotoxicity of non-irradiated and irradiated BSA-dsDNA51.7-AuNR as measured by an annexin V/PI assay. In a , b and c, results are expressed as Average ± SD (n=3).

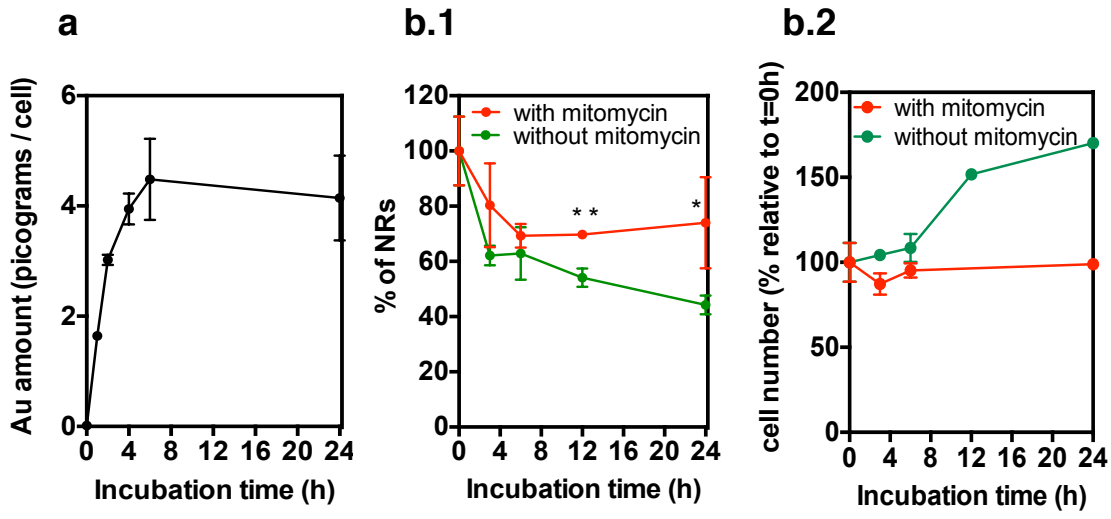

Figure S6. Uptake of β-Gal-dsDNA51.7-AuNR by fibroblasts. (a) Amount of Au in cells incubated with β-Gal-dsDNA51.7-AuNR (50 μg mL^{-1}) for different times. At each incubation time, cells were washed to remove the non-internalized AuNR after which they were trypsinized, counted and freeze-dried for ICP-MS analysis. (b) Amount of internalized Au during fibroblast proliferation. Cells were incubated with BSA-dsDNA68.9-AuNR (50 μg mL^{-1}) for 4 h, washed to remove the non-internalized AuNR, and cultured for additional 0, 3, 6, 12 and 24 h in cell culture media. In a set of experiments, cells were treated with mitomycin for 150 min after the 4 h uptake period. To determine the Au amount in the cells treated or not with mitomycin, cells were trypsinized, counted and freeze-dried for ICP-MS analysis. (b.1) Intracellular content of Au as quantified by ICP-MS. Unpaired t-test was used to compare both groups. * and ** mean $p<0.05$ and $p<0.01$. (b.2) Cell number relative to time 0 h (end of the incubation with NR). In a, b.1 and b.2, results are Average ± SD, n=3.

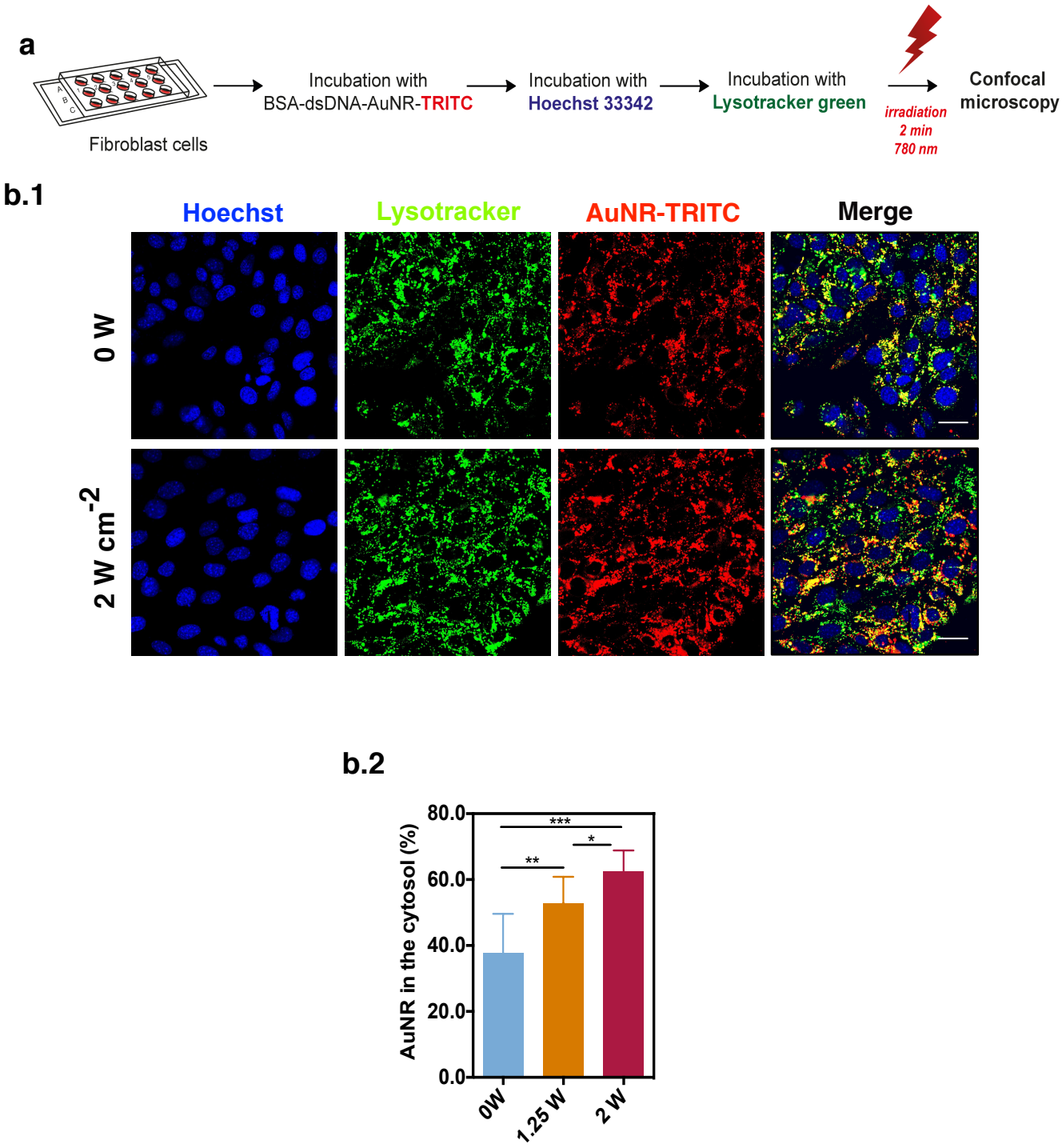

Figure S7. Intracellular trafficking of BSA-dsDNA51.7-AuNR-TRITC. (a) Schematic representation of the protocol used. (b.1) Confocal images of cells stained with lysotracker green after 4 h of incubation with BSA-dsDNA51.7-AuNR-TRITC (50 μg mL^{-1}) and laser irradiation (2 W cm^{-2}, 2 min). Scale bar is 30 µm. (b.2) Percentage of AuNR-TRITC outside the endolysosomal compartment, determined by calculating the overlap coefficient between TRITC and lysotracker green in ImageJ. Results are Average ± SD, n=9 (3 samples, 3 microscope fields per sample). *** denotes statistical significance ($p<0.001$) assessed by an unpaired t-test.

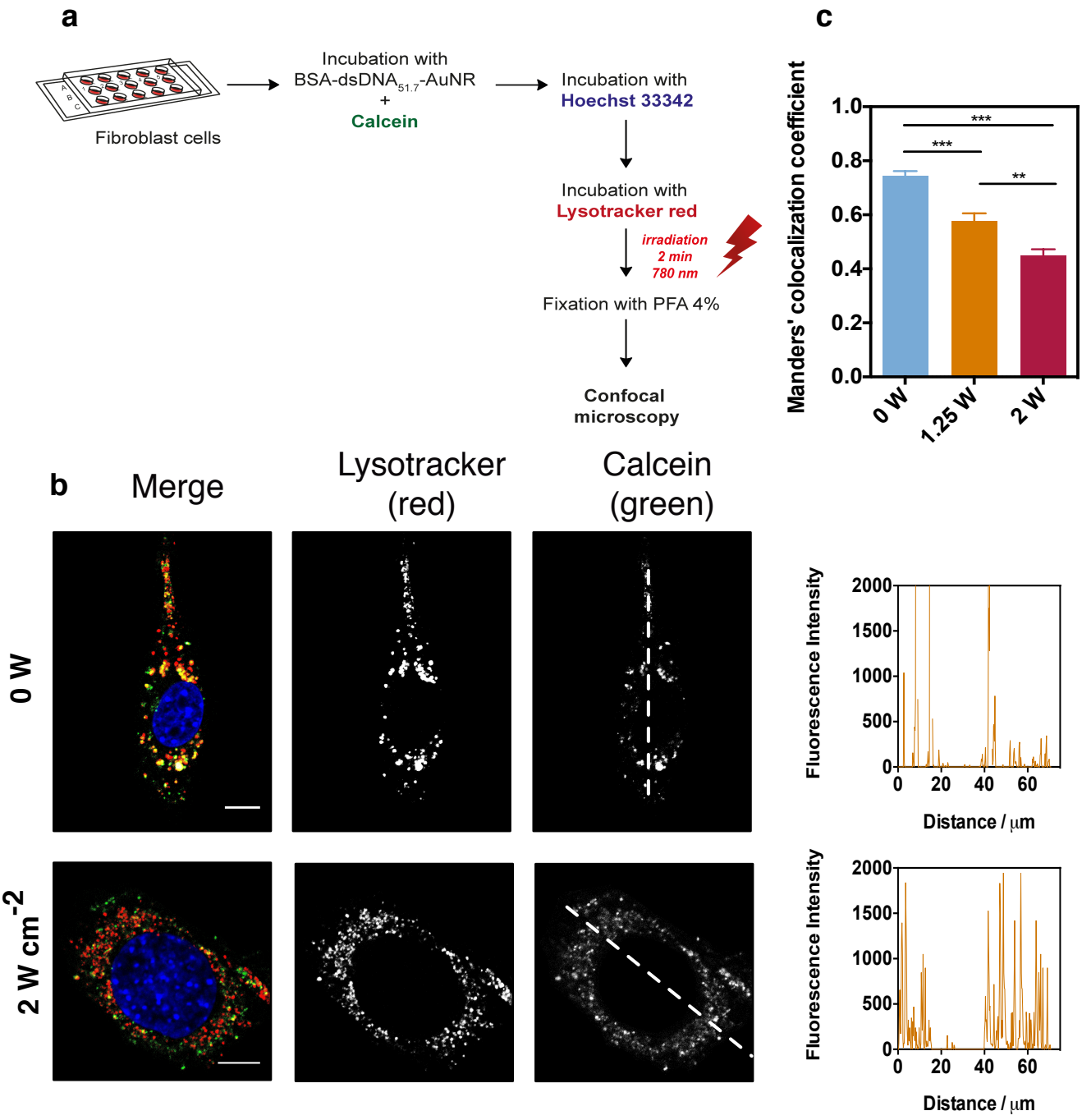

Figure S8. Effect of the NIR irradiation in the endolysomal escape of AuNRs. (a) Schematic representation of the protocol used. Cells were incubated with BSA-dsDNA51.7-AuNR (50 μg mL^{-1}) and calcein (25 mM) for 4 h. After replacing the medium, cells were incubated with lysotracker red (100 nM) for 15 min and then irradiated for 2 min with a laser at 780 nm (power: 1.25 or 2 W cm^{-2}). Cells were then observed in a confocal microscope. (b) Co-localization between calcein and lysotracker red in cells incubated with BSA-dsDNA51.7-AuNR. Scale bar 10 μm. Fluorescence intensity plots were obtained from cell regions labeled with a dash. (c) Co-localization between calcein and lysotracker red expressed as Manders' overlap coefficient (calculated using ImageJ). The results are expressed as Average ± SD, n=3 (3 samples, 4 microscope fields per sample). **, *** denote statistical significance ($p<0.01$; $p<0.001$) assessed by one-way ANOVA followed by Tukey's post-hoc test.

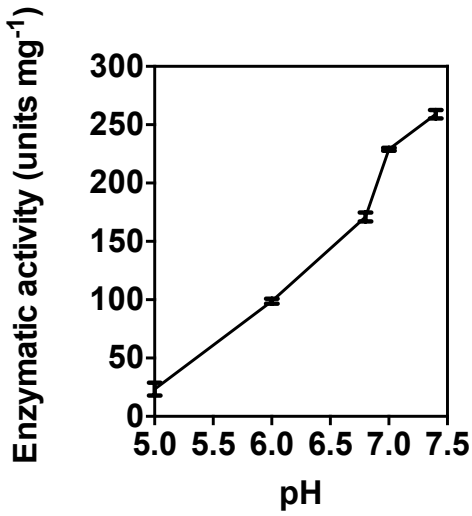

Figure S9. Enzymatic activity of β-Gal at different pHs. β-Gal (50 μL, 0.4 μg mL^{-1}) prepared in 0.1 M phosphate buffer (pH 5.0, 6.0, 6.8, 7.0 and 7.4) was added to ONPG (100 μL, 13 mg mL^{-1}) also prepared in 0.1 M phosphate buffer (pH 5.0, 6.0, 6.8, 7.0 and 7.4). The absorbance at 420 nm was measured for 30 min at 37 ºC in a 96 well plate using a Synergy HT microplate reader. One unit corresponds to the hydrolysis of 1 μmol of substrate (ONPG) per minute per mg of enzyme powder. The results are expressed as Average ± SD, n=3.

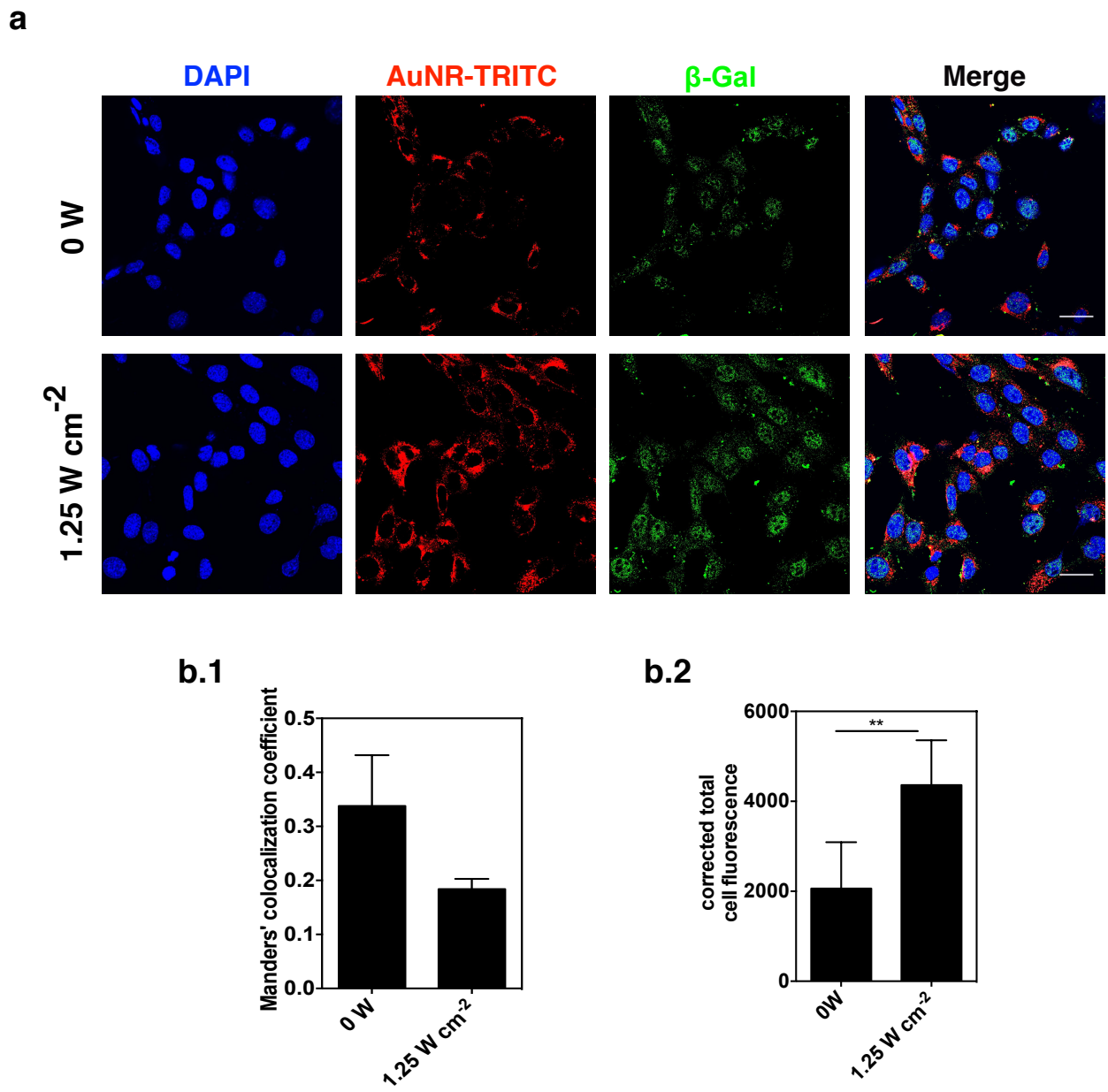

Figure S10. Intracellular levels of β-Gal assessed by immunocytochemistry. (a) Confocal images of fibroblasts incubated with βGal-dsDNA51.7-AuNR-TRITC. Cells were incubated for 4 h with βGal-dsDNA51.7-AuNR-TRITC (50 μg mL^{-1}), washed to remove the non-internalized AuNRs, feeded with new cell culture media and irradiated for 2 min with a 780 nm laser (power: 1.25 W cm^{-2}). Cells were fixed immediately after laser treatment (0 min) using a β-Gal antibody. Scale bar is 30 μm. (b.1) The co-localization between AuNR-TRITC and β-Gal was determined using ImageJ and is expressed as Manders' co-localization coefficient. After irradiation, and immediate (time 0 min) evaluation of the co-localization between β-Gal and AuNR-TRITC, our results show a decrease in the co-localization of both entities, which indicates the release of the protein from the AuNR. (b.2) Cell fluorescence in each experimental condition was corrected to the corresponding background fluorescence and thus designed as corrected total cell fluorescence. Results are Average ± SD, n=9 (3 samples, 3 microscope fields per sample). ** denotes statistical significance ($p<0.01$) assessed by an unpaired t-test.

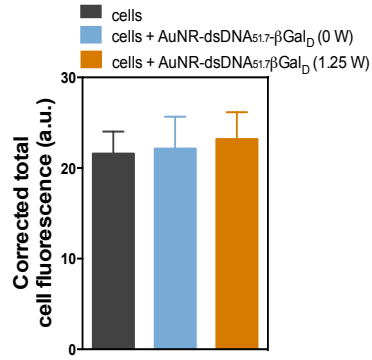

Figure S11. Enzymatic activity quantified after 4h of incubation with AuNRs conjugated with denatured β-Gal (AuNR-dsDNA51.7-βGalD) (50 μg mL^{-1}) followed by irradiation for 2 min at 1.25 W cm^{-2}. No significant change in the fluorescence was observed. Therefore, increase in the fluorescence requires an active enzyme (β-Gal). In a.2 and a.3, results are expressed as Average ± SD, n=3 (3 samples, 5 microscope fields per sample). **, *** denote statistical significance ($p<0.01$; $p<0.001$) assessed by one-way ANOVA followed by Tukey's post-hoc test.

Supplementary Data

Supplementary table 1. Oligonucleotide strands used for the conjugation to AuNRs and for protein modification. The melting temperature refers to a theoretical melting temperature relative to the portion of the strand that is able to hybridize with the complementary strand.

	Tm / ºC	sequence
AuNR conjugation	51.7	5'-HS-C6-TTTTTTTTTTTTTTTATAACTTCGTATA-3'
	68.9	5'-HS-C6-TTTTTTTTTTTTGTCCGGGTCCAGGGC-3'
DNA-protein conjugates	51.7	5'-HS-C6-TATACGAAGTTATAAAAAAAAAA-3'
	68.9	5'-HS-C6-TGCCCTGGACCCGGAC-3'

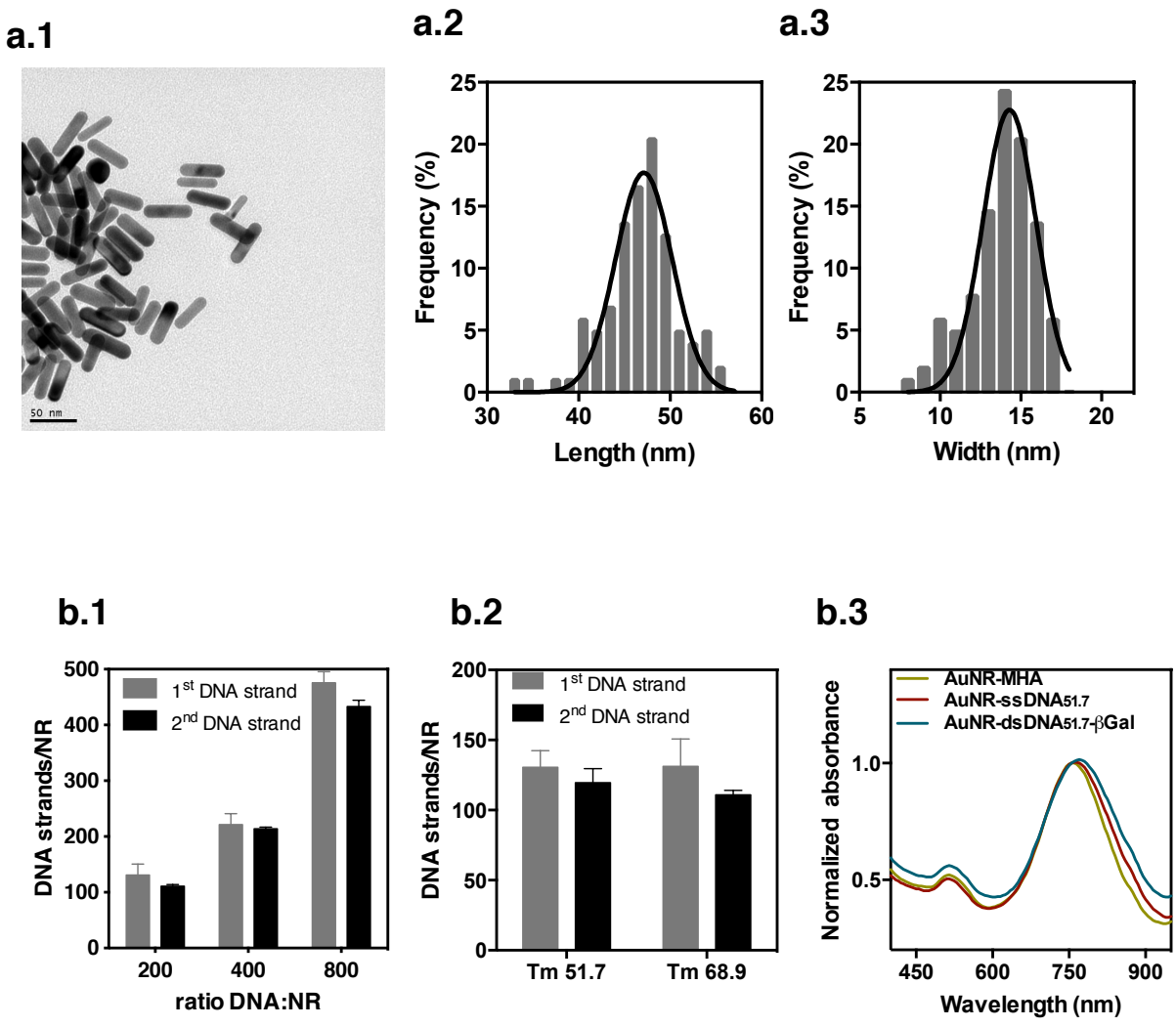

Figure S1. Characterization of AuNRs. (a) TEM analysis. (a.1) Representative TEM image of AuNRs. (a. 2-a.3) NR length (a.2) and width (a.3) distribution obtained from TEM images. The AuNRs showed an average length of 46.7 ± 4.1 nm, n=100 AuNRs and an average width of 13.8 ± 1.9 nm, n=100 AuNRs. (b.1) Quantification of oligonucleotides immobilized on NR surface via thiol gold chemistry (1st DNA strand) or hybridized to the ssDNA conjugated to the NR (2nd DNA strand). The amount of strands per AuNR was determined indirectly in the supernatant by measuring absorbance at 260 nm in Nanodrop. (b. 2) Comparison of the binding efficiency of the two sequences with different melting temperatures (91.7% efficiency for DNA strand with Tm 51.7 ºC and 84.5% efficiency for DNA strand with Tm 68.9 ºC). Results in b.1 and b.2 are Average ± SD, n=3. (b.3) Absorbance spectra of AuNRs after conjugation with mercaptohexanoic acid (AuNR-MHA); after conjugation with ssDNA51.7 (AuNR-ssDNA51.7) and after hybridization with β-Gal (AuNR-dsDNA51.7-βGal). Surface plasmon resonance band does not change significantly during surface modification.

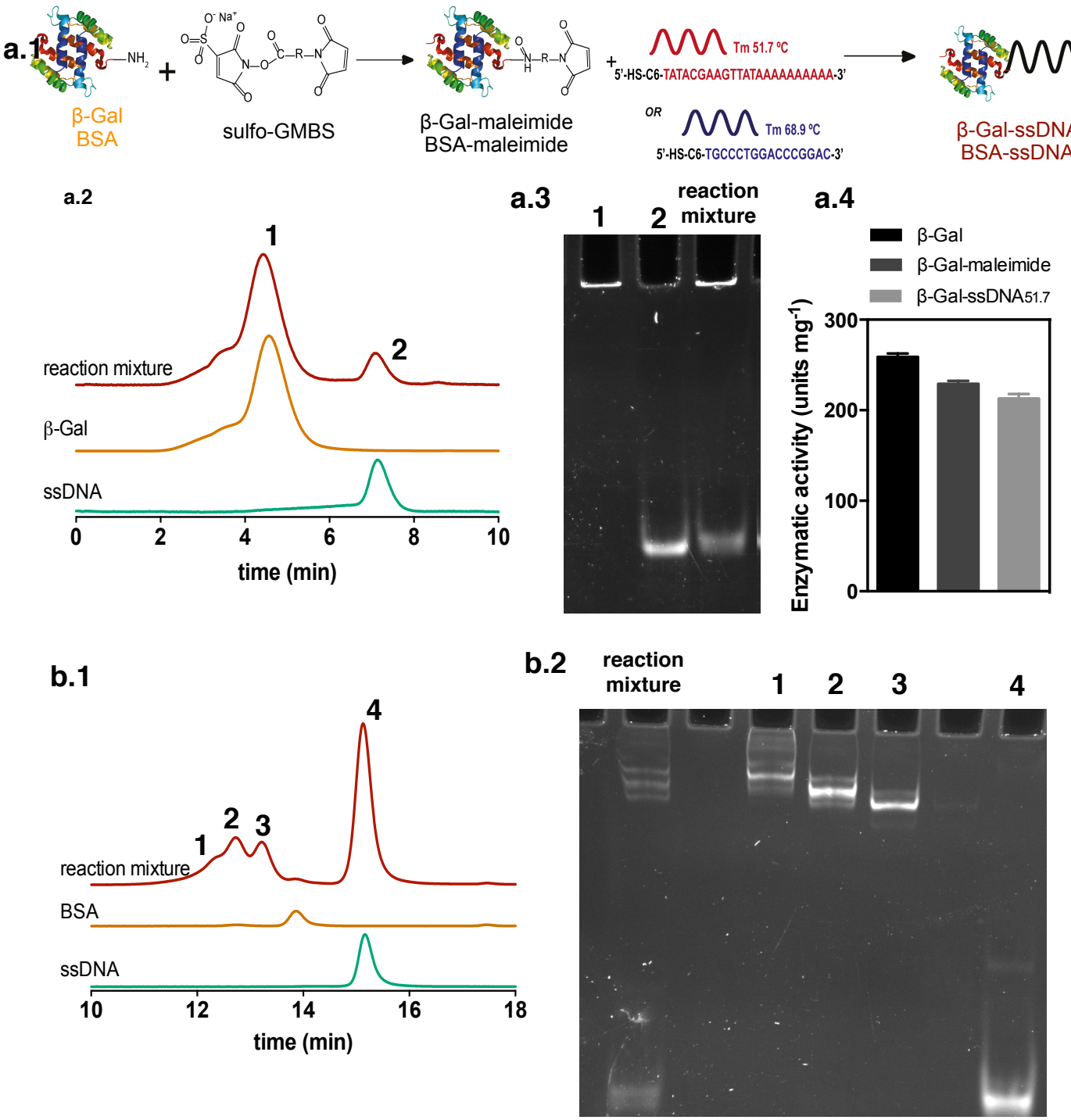

Figure S2. Characterization of oligonucleotide-protein conjugates. (a.1) Scheme showing the coupling reaction of ssDNA to the proteins. (a.2) HPLC characterization of the reaction mixture between β-Gal and ssDNA. Representative chromatograms of β-Gal, ssDNA and the final reaction mixture of β-Gal with ssDNA. Integration of DNA peaks indicate a conjugation value of 37% of the total DNA. This means that each protein molecule was conjugated with at least one oligonucleotide. (a.3) Electrophoresis characterization of the HPLC fractions. Fractions 1 and 2 were analysed. Samples were run in polyacrylamide gel and DNA (and not protein) was stained with Sybr Gold. Quantification of free DNA indicates a conjugation value of 35% of the total DNA. Fraction 1, which corresponds to the β-Gal-ssDNA conjugate was used for subsequent experiments. (a.4) Enzymatic activity β-Gal, β-Gal conjugated with sulfo-GMBS (β-Gal-maleimide) and β-Gal conjugated with ssDNA51.7 (β-Gal-ssDNA51.7). (b.1) HPLC characterization of the reaction mixture between BSA and ssDNA51.7. Representative chromatograms of BSA, ssDNA and the final reaction mixture of BSA with ssDNA. (b. 2) Electrophoresis characterization of the HPLC fractions. Fractions 1-4 were analyzed. Fraction 3 was used for conjugation with AuNR-ssDNA. We selected this fraction because each protein is conjugated with one ssDNA.

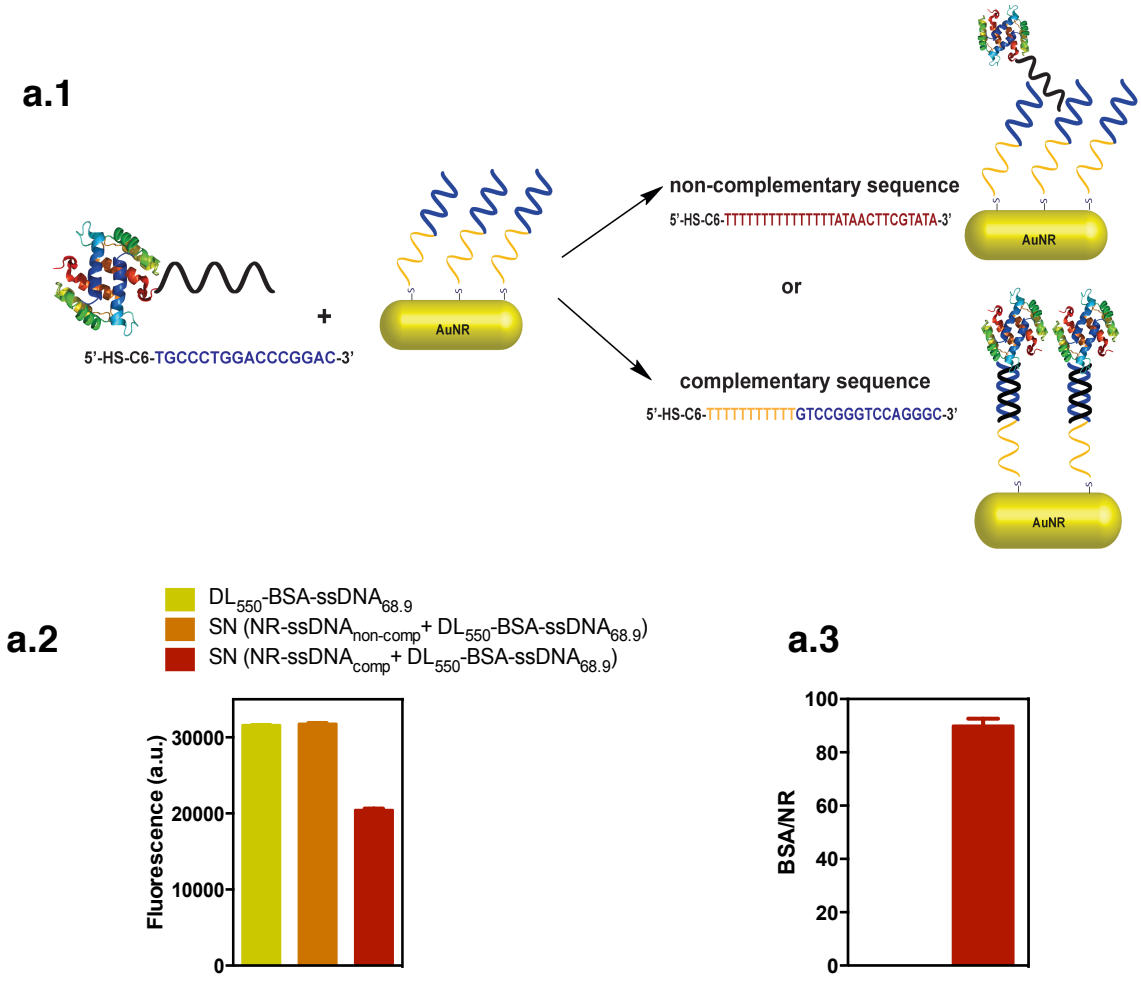

Figure S3. Specificity for the hybridization between AuNR-ssDNA and BSA-ssDNA. (a.1) Scheme showing the experiment set-up to demonstrate that the hybridization between AuNR-ssDNA68.9 and BSA-ssDNA68.9 was specific. (a.2) Fluorescence intensity of the supernatants collected after the hybridization of DL550-BSA-ssDNA68.9 to AuNRs conjugated with complementary (ssDNAcomp) or non-complementary (ssDNAnon-comp) oligonucleotide sequences. The ratio BSA to AuNRs was 1:300. DL550-BSA-ssDNA68.9 solution for hybridization was used as a control. (a.3) Number of proteins immobilised per AuNR, calculated indirectly from the fluorescence in the supernatant through a calibration curve (concentration between 2.5 and 50 nM, excitation at 480 nm and emission at 515 nm). In a.2 and a.3, results are Average ± SD, n=3.

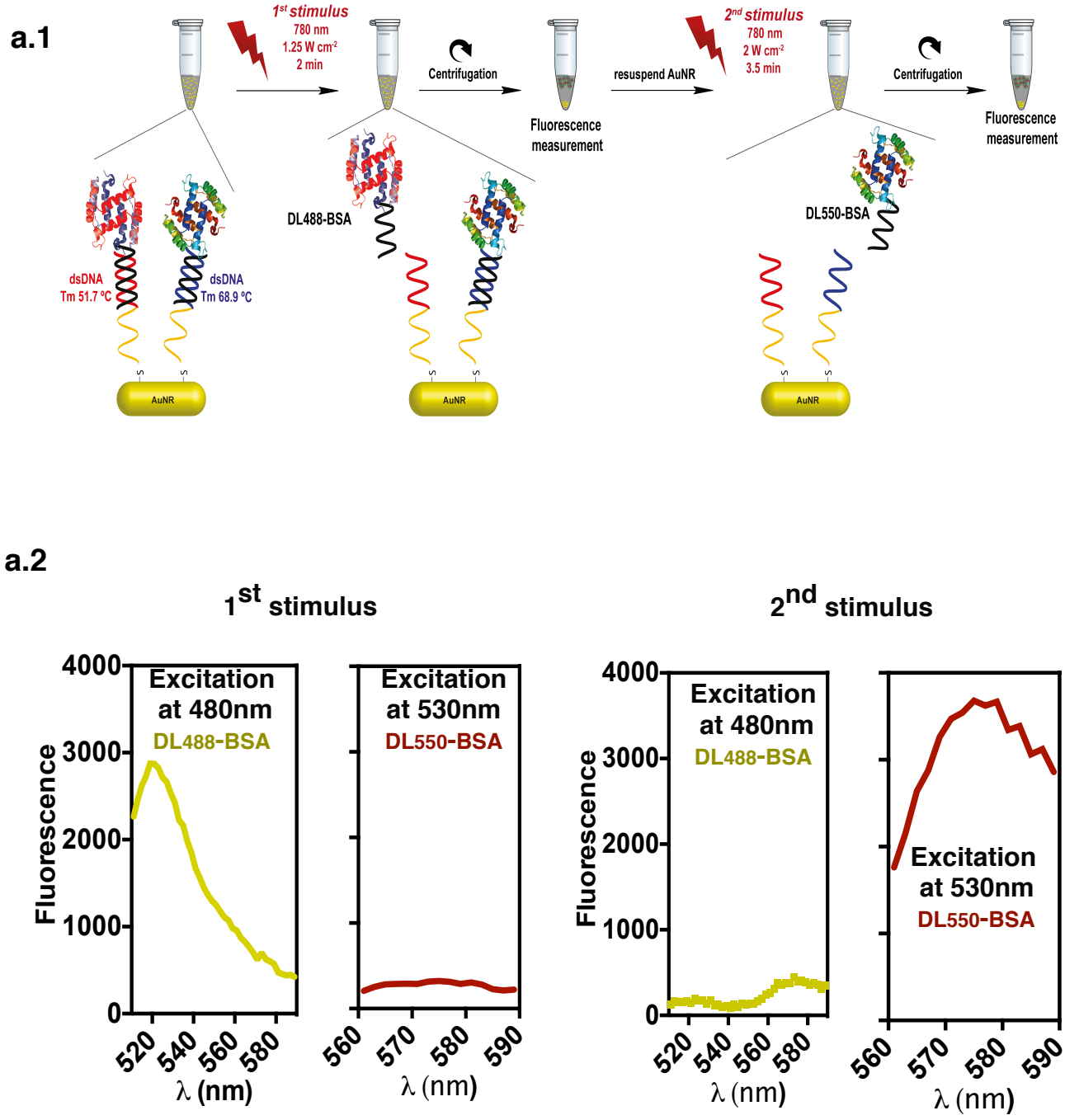

Figure S4. Sequential release of DL488-BSA-ssDNA51.7 and DL550-BSA-ssDNA68.9 from AuNRs after light activation. (a.1) Scheme illustrating dual release experiment. A suspension of DL488-BSA-dsDNA51.7-AuNR-DL550-BSA-dsDNA68.9 was first irradiated for 2 min at 1.25 W cm^{-2} and then centrifuged in order to collect the supernatant. The NR were resuspended and irradiated again at 2 W cm^{-2} for 3.5 min and then centrifuged. AuNRs used in this experiment were conjugated with 32 molecules of DL488-BSA-ssDNA51.7 and 34 molecules of DL550-BSA-ssDNA68.9. (a.2) The fluorescence of both supernatants was measured in a fluorimeter using an excitation wavelength at 480 nm for DL488-BSA or 530 nm for DL550-BSA. The first stimulus caused the release of 86% of DL488-BSA and 7% of DL550-BSA. The second stimulus released 14% of DL488-BSA and 93% of DL550-BSA.

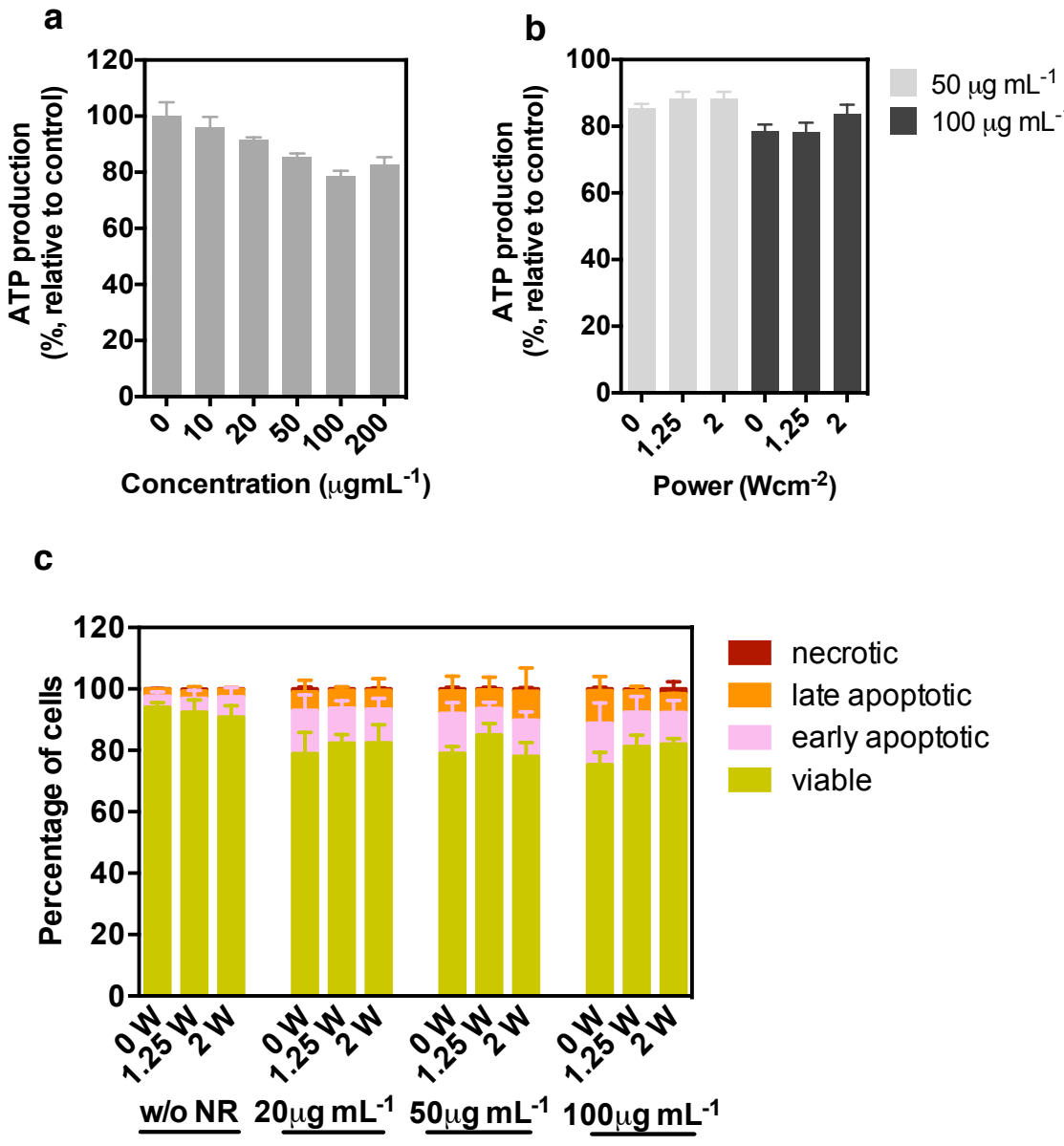

Figure S5. Cytotoxicity of BSA-dsDNA51.7-AuNR. Fibroblasts were incubated with different concentrations of BSA-dsDNA51.7-AuNR for 4 h, washed, incubated in cell culture media for 20 h after which cell metabolism (a and b) or cell viability (c) was evaluated by an ATP (a and b) or annexin V/PI (c) assays. Control are cells cultured without AuNRs. (a and b) Cytotoxicity of non-irradiated BSA-dsDNA51.7-AuNR (a) and irradiated BSA-dsDNA51.7-AuNR (780 nm laser for 2 min; laser powers: 1.25 and 2 W cm^{-2}) (b) as evaluated by an ATP assay. (c) Cytotoxicity of non-irradiated and irradiated BSA-dsDNA51.7-AuNR as measured by an annexin V/PI assay. In a , b and c, results are expressed as Average ± SD (n=3).

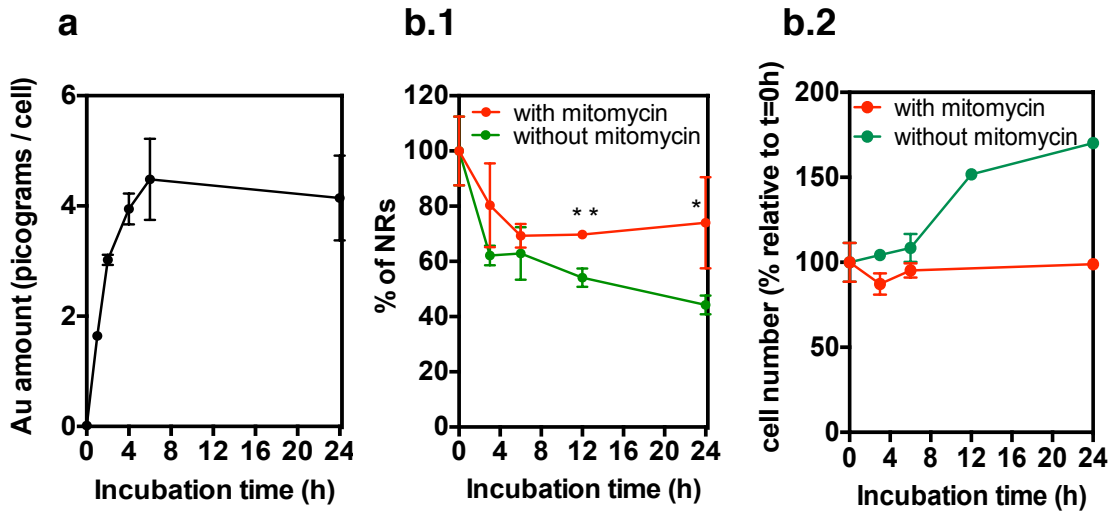

Figure S6. Uptake of β-Gal-dsDNA51.7-AuNR by fibroblasts. (a) Amount of Au in cells incubated with β-Gal-dsDNA51.7-AuNR (50 μg mL^{-1}) for different times. At each incubation time, cells were washed to remove the non-internalized AuNR after which they were trypsinized, counted and freeze-dried for ICP-MS analysis. (b) Amount of internalized Au during fibroblast proliferation. Cells were incubated with BSA-dsDNA68.9-AuNR (50 μg mL^{-1}) for 4 h, washed to remove the non-internalized AuNR, and cultured for additional 0, 3, 6, 12 and 24 h in cell culture media. In a set of experiments, cells were treated with mitomycin for 150 min after the 4 h uptake period. To determine the Au amount in the cells treated or not with mitomycin, cells were trypsinized, counted and freeze-dried for ICP-MS analysis. (b.1) Intracellular content of Au as quantified by ICP-MS. Unpaired t-test was used to compare both groups. * and ** mean $p<0.05$ and $p<0.01$. (b.2) Cell number relative to time 0 h (end of the incubation with NR). In a, b.1 and b.2, results are Average ± SD, n=3.

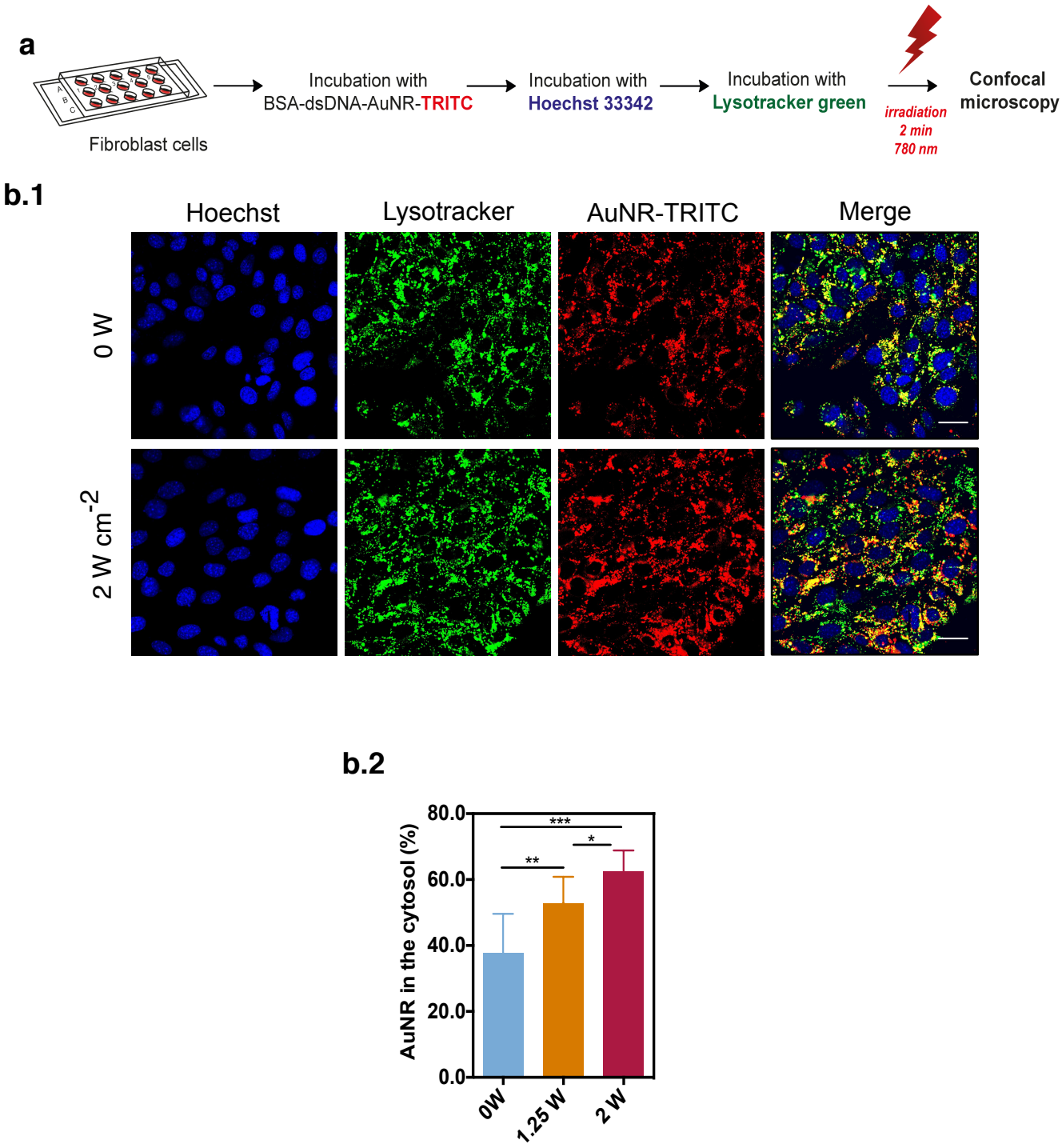

Figure S7. Intracellular trafficking of BSA-dsDNA51.7-AuNR-TRITC. (a) Schematic representation of the protocol used. (b.1) Confocal images of cells stained with lysotracker green after 4 h of incubation with BSA-dsDNA51.7-AuNR-TRITC (50 μg mL^{-1}) and laser irradiation (2 W cm^{-2}, 2 min). Scale bar is 30 µm. (b.2) Percentage of AuNR-TRITC outside the endolysosomal compartment, determined by calculating the overlap coefficient between TRITC and lysotracker green in ImageJ. Results are Average ± SD, n=9 (3 samples, 3 microscope fields per sample). *** denotes statistical significance ($p<0.001$) assessed by an unpaired t-test.

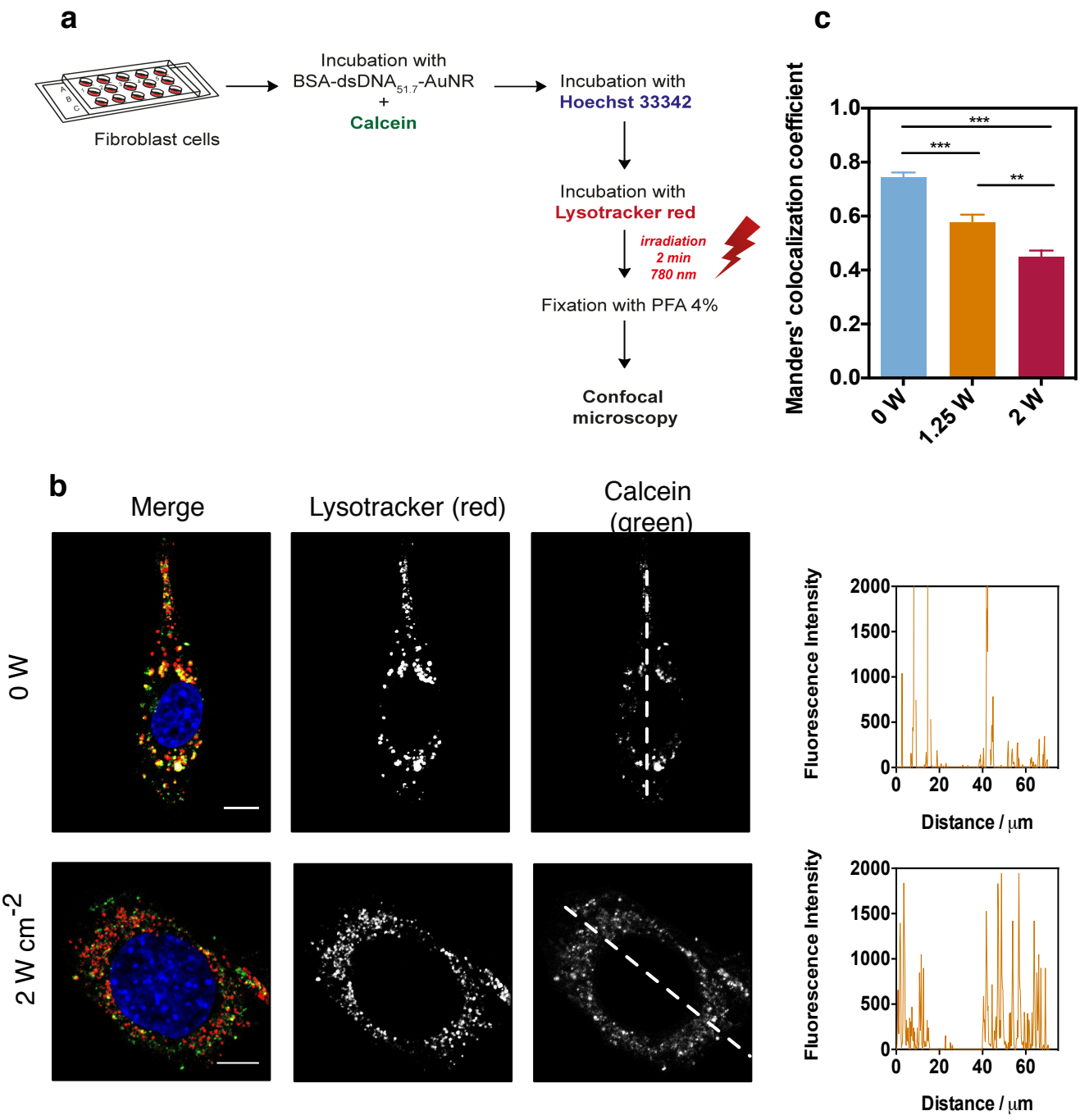

Figure S8. Effect of the NIR irradiation in the endolysomal escape of AuNRs. (a) Schematic representation of the protocol used. Cells were incubated with BSA-dsDNA51.7-AuNR (50 μg mL^{-1}) and calcein (25 mM) for 4 h. After replacing the medium, cells were incubated with lysotracker red (100 nM) for 15 min and then irradiated for 2 min with a laser at 780 nm (power: 1.25 or 2 W cm^{-2}). Cells were then observed in a confocal microscope. (b) Co-localization between calcein and lysotracker red in cells incubated with BSA-dsDNA51.7-AuNR. Scale bar 10 μm. Fluorescence intensity plots were obtained from cell regions labeled with a dash. (c) Co-localization between calcein and lysotracker red expressed as Manders' overlap coefficient (calculated using ImageJ). The results are expressed as Average ± SD, n=3 (3 samples, 4 microscope fields per sample). **, *** denote statistical significance ($p<0.01$; $p<0.001$) assessed by one-way ANOVA followed by Tukey's post-hoc test.

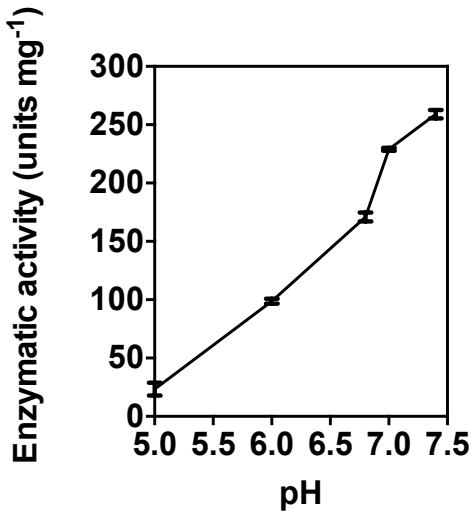

Figure S9. Enzymatic activity of β-Gal at different pHs. β-Gal (50 μL, 0.4 μg mL^{-1}) prepared in 0.1 M phosphate buffer (pH 5.0, 6.0, 6.8, 7.0 and 7.4) was added to ONPG (100 μL, 13 mg mL^{-1}) also prepared in 0.1 M phosphate buffer (pH 5.0, 6.0, 6.8, 7.0 and 7.4). The absorbance at 420 nm was measured for 30 min at 37 ºC in a 96 well plate using a Synergy HT microplate reader. One unit corresponds to the hydrolysis of 1 μmol of substrate (ONPG) per minute per mg of enzyme powder. The results are expressed as Average ± SD, n=3.

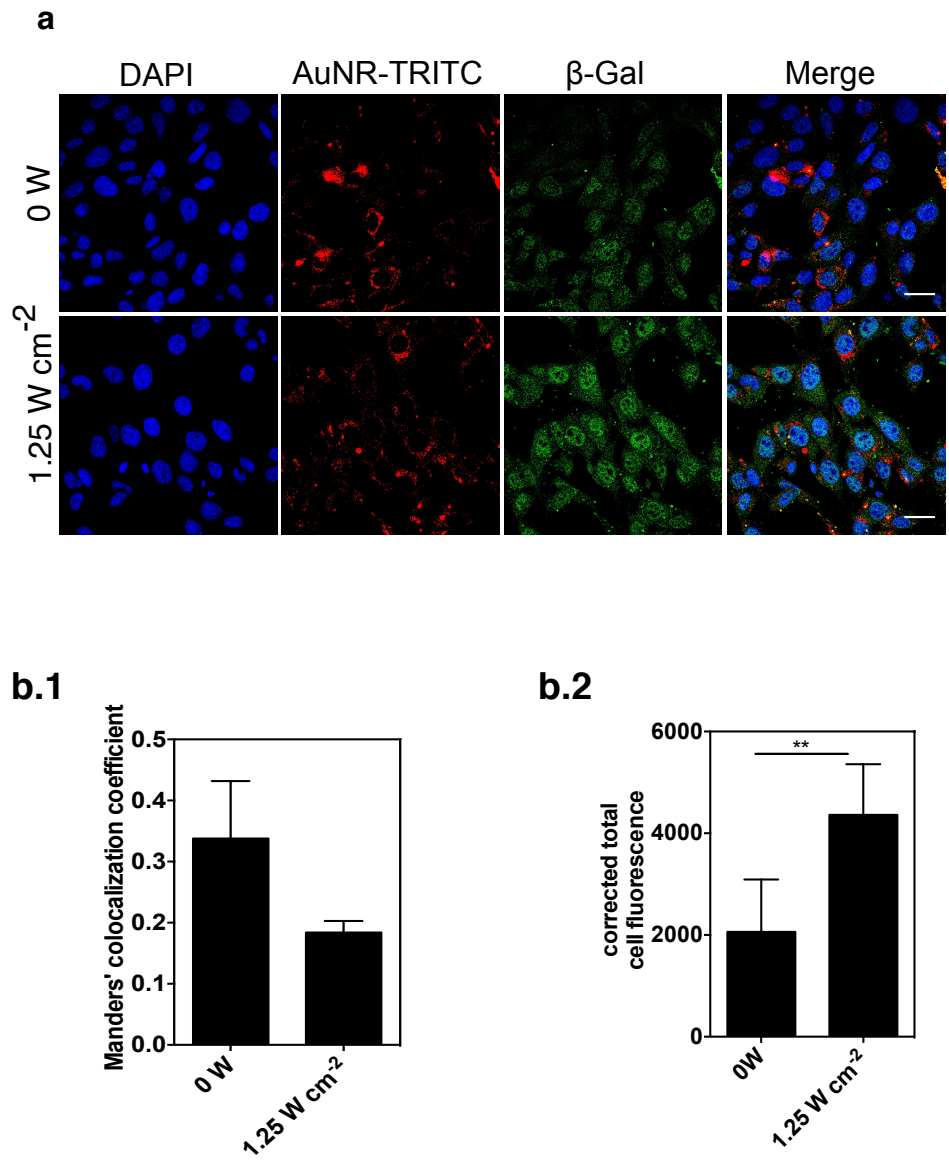

Figure S10. Intracellular levels of β-Gal assessed by immunocytochemistry. (a) Confocal images of fibroblasts incubated with βGal-dsDNA51.7-AuNR-TRITC. Cells were incubated for 4 h with βGal-dsDNA51.7-AuNR-TRITC (50 μg mL^{-1}), washed to remove the non-internalized AuNRs, feeded with new cell culture media and irradiated for 2 min with a 780 nm laser (power: 1.25 W cm^{-2}). Cells were fixed immediately after laser treatment (0 min) using a β-Gal antibody. Scale bar is 30 μm. (b.1) The co-localization between AuNR-TRITC and β-Gal was determined using ImageJ and is expressed as Manders' co-localization coefficient. After irradiation, and immediate (time 0 min) evaluation of the co-localization between β-Gal and AuNR-TRITC, our results show a decrease in the co-localization of both entities, which indicates the release of the protein from the AuNR. (b.2) Cell fluorescence in each experimental condition was corrected to the corresponding background fluorescence and thus designed as corrected total cell fluorescence. Results are Average ± SD, n=9 (3 samples, 3 microscope fields per sample). ** denotes statistical significance ($p<0.01$) assessed by an unpaired t-test.

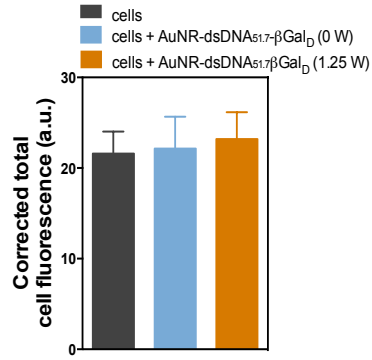

Figure S11. Enzymatic activity quantified after 4h of incubation with AuNRs conjugated with denatured β-Gal (AuNR-dsDNA51.7-βGalD) (50 μg mL^{-1}) followed by irradiation for 2 min at 1.25 W cm^{-2}. No significant change in the fluorescence was observed. Therefore, increase in the fluorescence requires an active enzyme (β-Gal). In a.2 and a.3, results are expressed as Average ± SD, n=3 (3 samples, 5 microscope fields per sample). **, *** denote statistical significance ($p<0.01$; $p<0.001$) assessed by one-way ANOVA followed by Tukey's post-hoc test.